Reconstructing Sign-Changing Dark Energy Density: From Data to Fundamental Theory

N.Katirci
Doğuş University / ISTANBUL

$$\mathcal{M}^{1+3+n} = \mathcal{R} \times M^3 \times \mathcal{K}$$

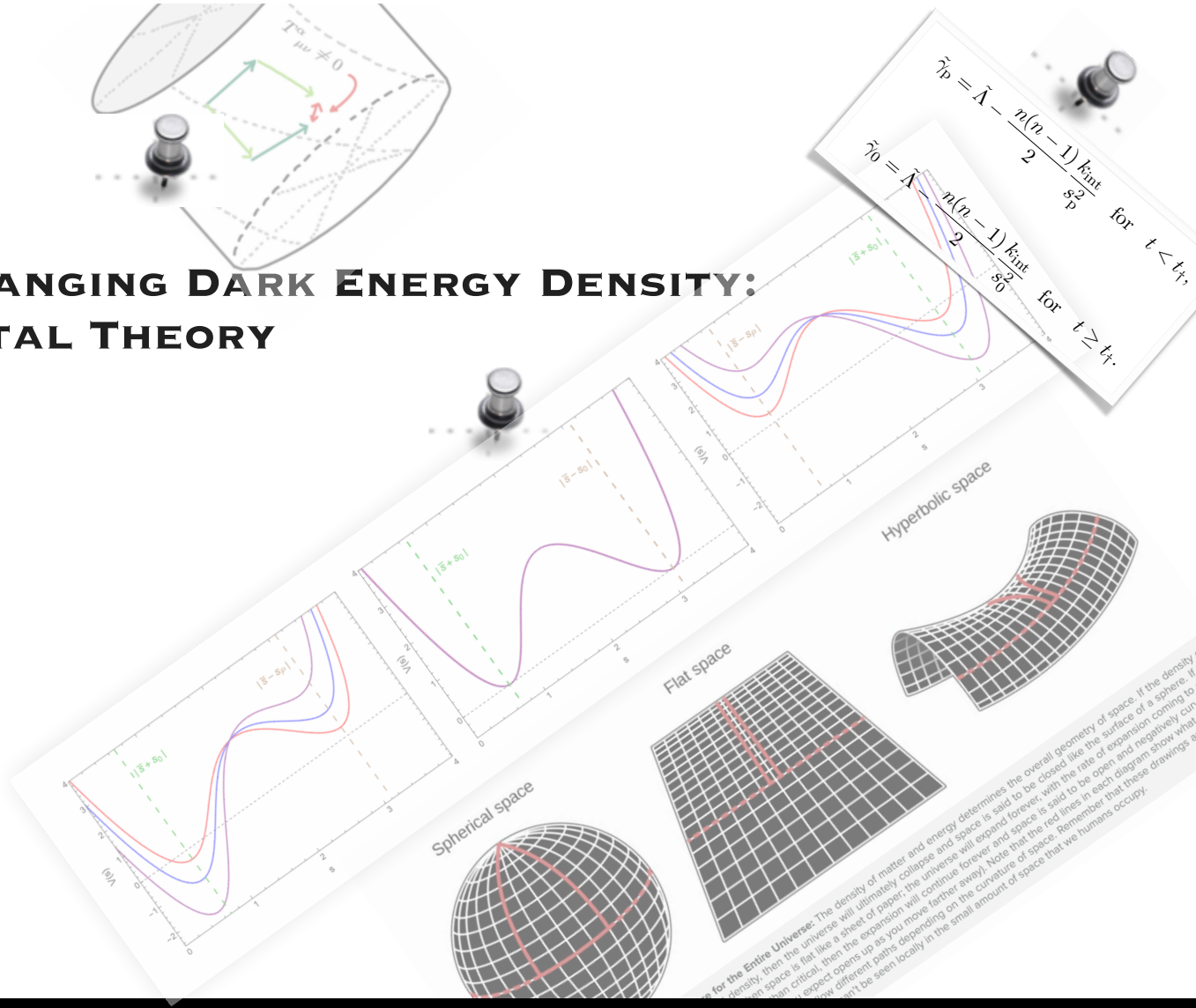

PASCOS 2026, the 31st International Symposium on Particles, Strings, and Cosmology,
Sheffield University, Richard Roberts Auditorium
22-26 June 2026

Hubble (H_0) Tension

Model dependent (Indirect) measurement

The Planck estimate assuming a "vanilla" ΛCDM cosmological model:

H_0 = 67.36 ‡ 0.54 km/s/Mpc

Planck 2018, Astron. Astrophys. 641 (2020) A6

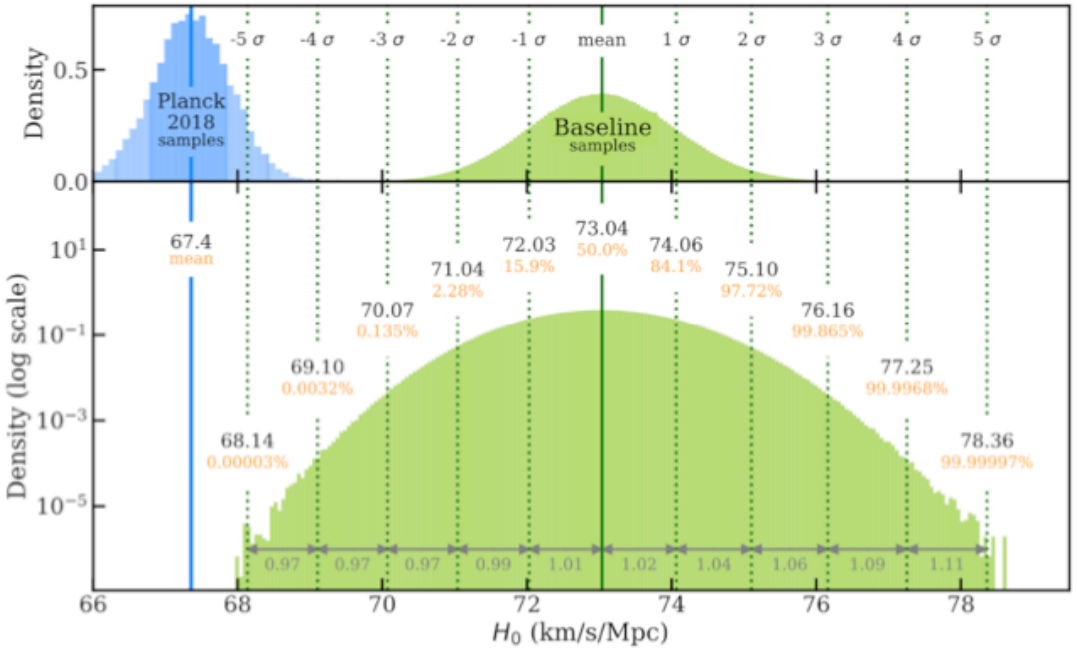

±5σ : one in 3.5 million implausible to reconcile the two by chance

In the recent SPT-3G D1 analysis (arXiv:2506.207079), the combined CMB data sets (SPA = Planck + SPT + ACT) yields an H0 tension in ΛCDM exceeding 6σ.

Casertano et al.[HODN],
The Local Distance Network: A community consensus report on the measurement of the Hubble constant at 1% precision,
Astron. Astrophys. 708 (2026), A166
arXiv:2510.23823

This paper measured the local H_0 not by relying on a single team (e.g. SH0ES) but by combining dozens of independent distance indicators (Cepheids, TRGB, SN Ia, masers, SBF, etc.) within a covariance-weighted "Distance Network" community consensus, yielding ***H_0 = 73.50 ± 0.81*** (about 1% precision). Its significance: the Hubble tension can no longer be easily blamed on one group's method or a possible systematic error, since the "~73" local value is now firmly established by a broad, independent community.

Model independent (direct) measurement

The latest local measurements obtained by the SH0ES collaboration

Riess et al. Astrophys.J.Lett. 934 (2022) 1 L7.

H_0 =73.04±1.04 km/s/Mpc.

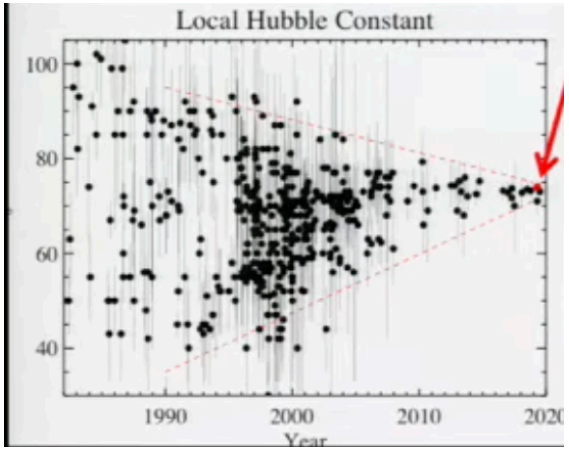

A.RIESS

ΛCDM: Much More Than We Expected, but Now Less Than What We Want
Michael S. Turner
Foundations of Physics 48 (10):1261-1278 (2018)

Physics of the Dark Universe 49 (2025) 101965

Contents lists available at ScienceDirect

Physics of the Dark Universe

journal homepage: www.elsevier.com/locate/dark

Review article

The CosmoVerse White Paper: Addressing observational tensions in cosmology with systematics and fundamental physics

Eleonora Di Valentino [1], Jackson Levi Said [2 3], Adam Riess [4 5], Agnieszka Pollo [6], Vivian Poulin [7], Adrià Gómez-Valent [8], Amanda Weltman [9], Antonella Palmese [10], Caroline D. Huang [11], Carsten van de Bruck [12], Chandra Shekhar Saraf [13], Cheng-Yu Kuo [14], Cora Uhlemann [15 16], Daniela Grandón [17], Dante Paz [18], Dominique Eckert [19], Elsa M. Teixeira [20], Emmanuel N. Saridakis [21 22 23], Eoin Ó Colgáin [24], Florian Beutler [25]...Zahra Davari [543]

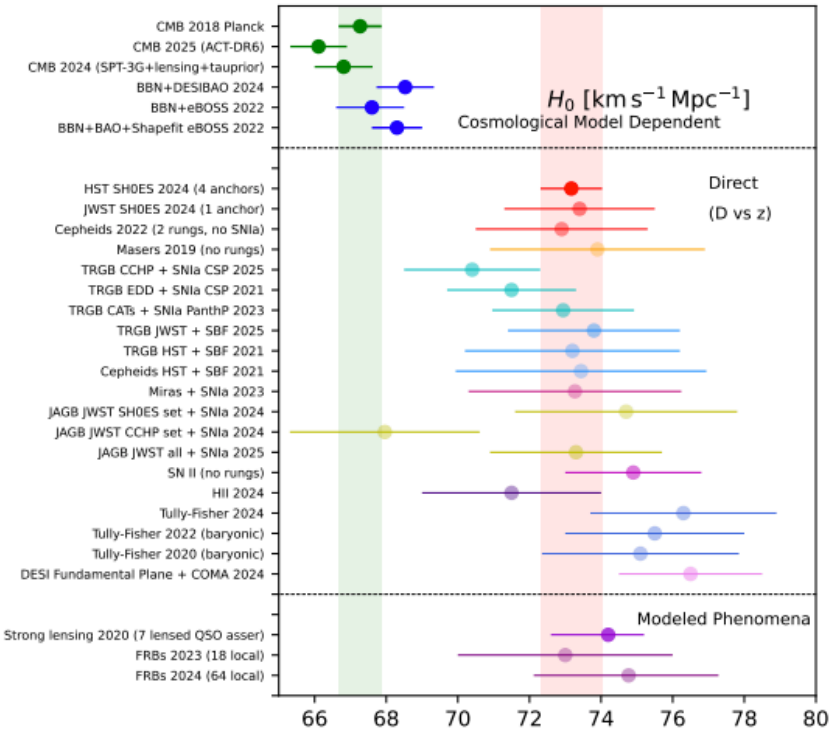

FIG. 1: Summary of H_0 estimates from different cosmological probes with error bars smaller than $3.5\,\mathrm{km\,s^{-1}\,Mpc^{-1}}$.

ded a good phenomenological description of a wide range of observations both at astroj
d is constructed by a universal cosmological constant and supported by a matter sector
ontribution, as well as very early-time inflationary physics, and underpinned by gravit
out the soundness of the foundations of the standard model. However, recent years hav
h the emergence of differences between certain cosmological probes. In this White Pape
; decade together with the core science projects that aim to meet these challenges. Th
core cosmological parameters with varying levels of statistical confidence. These pos
rious measurements or cosmological probes but there is also a growing indication of p
pal probes used in the measurement of cosmological parameters, as well as potential s
at may be observable in upcoming surveys. We also discuss the growing set of novel
l models. These new methods will become increasingly important in the coming yea
cy between predictions of different physical models grows. There are several perspecti
ch as the model-independent probes in the late Universe and model-dependent meas
r closes with a number of recommendations for the community to focus on for the up
ndamental physics developments.

ANOMALIES & TENSIONS IN COSMOLOGY • COSMOVERSE •

out of the CosmoVerse COST
g observational tensions in cos-
ital physics [1,2]), which traces
fort in the cosmic tensions sec-
deliverables of the COST Action
n of this network is to establish
across the disparate themes of

observational cosmology, novel technique
mental physics. This White Paper demonst
successful, while also laying out a roadma
expand the interdisciplinary nature of the
of the community. Another core aspect
approaches between the constituent subc
common language in which to discuss the
In the White Paper, the accomplishm
strated through the interwoven connect
munities of the network and the granul
through a diverse set of actions, includi

11

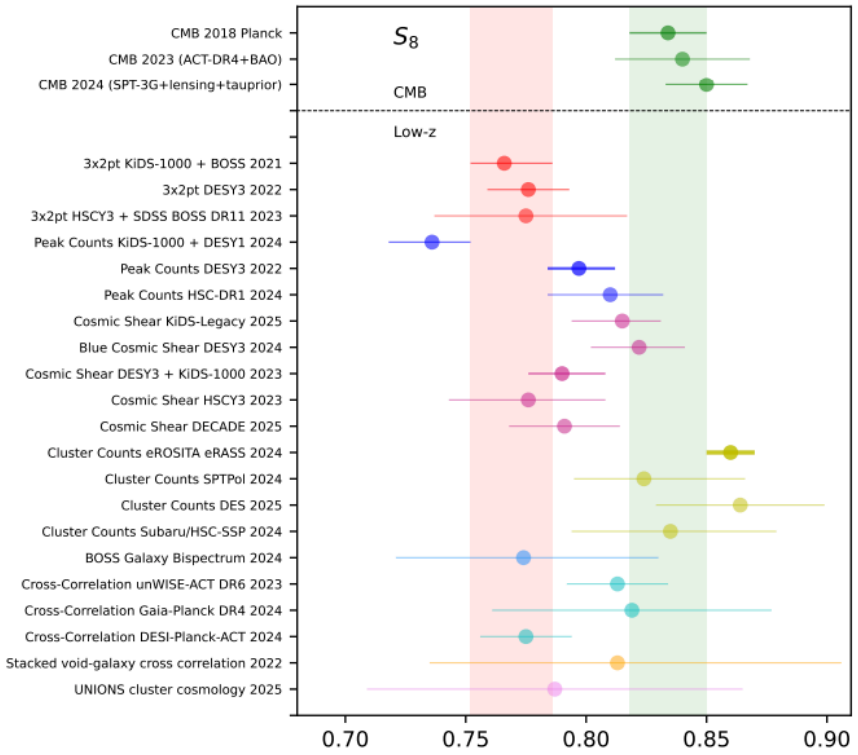

FIG. 4: Summary of S_8 estimates from different cosmological probes.

Λ_sCDM

Rastall extension of GR EPJC 80, 1050 (2020). 2004.04074]
Brans Dicke extension of GR EPJC 80 (2020) 32, 1903.06679]

an idea that grew out of the earlier "graduated dark energy" (gDE) work, where a spontaneous sign switch first appeared as an observational hint rather than an imposed feature.

Akarsu barrow Escamilla Vazquez , Phys. Rev. D 101, 063528 (2020), 1912.08751

Cosmological Constant
or the usual vacuum energy of QFT

$$\varrho_\Lambda = 0$$

Simple-gDE:

$$\varrho = \text{constant}$$

Acquaviva, Akarsu, Katırcı & Vazquez
PRD (2021), arXiv:2104.02623

gDE: Graduated dark energy

$$\varrho = \gamma\rho_0 \left(\frac{\rho}{\rho_0}\right)^\lambda$$

The simplest dynamical deviation from zero inertial mass density of the usual vacuum energy density. Inspired by *Graduated inflationary universes*, Barrow, PLB, 1990.

$$\frac{H^2}{H_0^2} = \Omega_{r0}(1+z)^4 + \Omega_{m0}(1+z)^3 + \Omega_{\Lambda_s 0}\,\mathrm{sgn}[z_\dagger - z]$$

$$\lambda \to -\infty$$

$$\varrho \propto \rho^\lambda < 0 \quad \text{with} \quad \lambda < 1$$

its energy density dynamically takes negative values in the finite past.

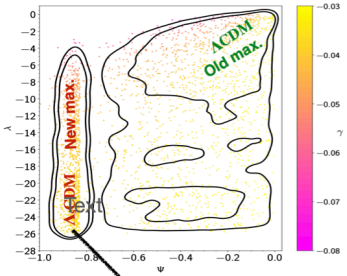

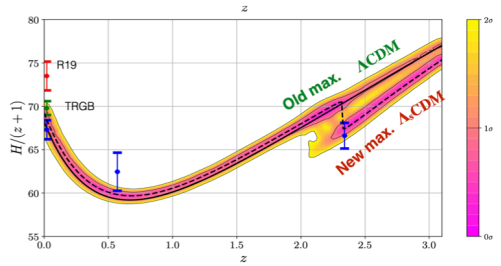

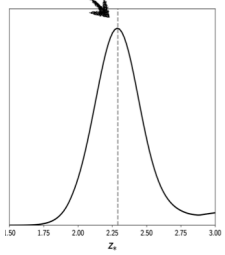

11

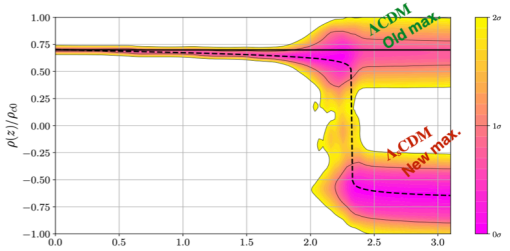

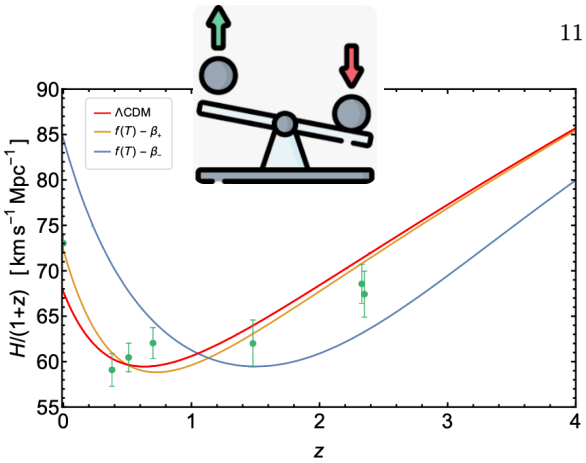

Akarsu, Özülker, Kumar & Vazquez
Phys. Rev. D 104, 123512 (2021),2108.09239

Akarsu, Kumar, Vazquez & Yadav
Phys. Rev. D 108, 023513 (2023), 2211.05742

Akarsu, Di Valentino, Kumar, Nunes, Vazquez, Yadav
2307.10899

First indications towards dark energy with negative energy density values at high redshifts

Rastall extension of GR EPJC 80, 1050 (2020) 2004.04074] & Brans Dicke extension of GR EPJC 80 (2020) 32, 1903.06679]

Cosmological implications of baryon acoustic oscillation (BAO) measurements

Éric Aubourg[1], Stephen Bailey[2], Julian E. Bautista[1], Florian Beutler[2], Vaishali Bhardwaj[3,2], Dmitry Bizyaev[4], Michael Blanton[5], Michael Blomqvist[6], Adam S. Bolton[7], Jo Bovy[8], Howard Brewington[4], J. Brinkmann[4], Joel R. Brownstein[7], Angela Burden[9], Nicolás G. Busca[1,10,11], William Carithers[2], Chia-Hsun Chuang[12], Johan Comparat[12], Rupert A.C. Croft[13,14], Antonio J. Cuesta[15,16], Kyle S. Dawson[7], Timothée Delubac[17], Daniel J. Eisenstein[18], Andreu Font-Ribera[2], Jian Ge[19], J.-M. Le Goff[20], Satya Gontcho A Gontcho[16], J. Richard Gott, III[21], James E. Gunn[21], Hong Guo[22,7], Julien Guy[23,2], Jean-Christophe Hamilton[1], Shirley Ho[13], Klaus Honscheid[24,25], Cullan Howlett[9], David Kirkby[6], Francisco S. Kitaura[26], Jean-Paul Kneib[17,27], Khee-Gan Lee[28], Dan Long[4], Robert H. Lupton[21], Mariana Vargas Magaña[1], Viktor Malanushenko[4], Elena Malanushenko[4], Marc Manera[9,29], Claudia Maraston[9], Daniel Margala[6], Cameron K. McBride[18], Jordi Miralda-Escudé[30,16], Adam D. Myers[31], Robert C. Nichol[9], Pasquier Noterdaeme[32], Sebastián E. Nuza[26], Matthew D. Olmstead[7], Daniel Oravetz[4], Isabelle Pâris[33], Nikhil Padmanabhan[15], Nathalie Palanque-Delabrouille[2,20], Kaike Pan[4], Marcos Pellejero-Ibanez[34,35], Will J. Percival[9], Patrick Petitjean[32], Matthew M. Pieri[36], Francisco Prada[12,37,38], Beth Reid[2,39], James Rich[20], Natalie A. Roe[2], Ashley J. Ross[9,25], Nicholas P. Ross[40], Graziano Rossi[41,20], Jose Alberto Rubiño-Martín[34,35], Ariel G. Sánchez[42], Lado Samushia[43,44], Ricardo Tanausú Génova Santos[34], Claudia G. Scóccola[12,34,45], David J. Schlegel[2], Donald P. Schneider[46,47], Hee-Jong Seo[25,48], Erin Sheldon[49], Audrey Simmons[4], Ramin A. Skibba[50], Anže Slosar[49], Michael A. Strauss[21], Daniel Thomas[9], Jeremy L. Tinker[5], Rita Tojeiro[9], Jose Alberto Vazquez[49], Matteo Viel[33,51], David A. Wake[52,53], Benjamin A. Weaver[5], David H. Weinberg[25,54], W. M. Wood-Vasey[55], Christophe Yèche[20], Idit Zehavi[56], and Gong-Bo Zhao[57,9]
(Dated: October 12, 2015. Authors' institutions can be found in Appendix A.)

We derive constraints on cosmological parameters and tests of dark energy models from the combination of baryon acoustic oscillation (BAO) measurements with cosmic microwave background (CMB) data and a recent reanalysis of Type Ia supernova (SN) data. In particular, we take advantage of high-precision BAO measurements from galaxy clustering and the Lyman-α forest (LyaF) in the SDSS-III Baryon Oscillation Spectroscopic Survey (BOSS). Treating the BAO scale as an uncalibrated standard ruler, BAO data alone yield a high confidence detection of dark energy; in combination with the CMB angular acoustic scale they further imply a nearly flat universe. Adding the CMB-calibrated physical scale of the sound horizon, the combination of BAO and SN data into an "inverse distance ladder" yields a measurement of $H_0 = 67.3 \pm 1.1\,\mathrm{km\,s^{-1}\,Mpc^{-1}}$, with 1.7% precision. This measurement assumes standard pre-recombination physics but is insensitive to assumptions about dark energy or space curvature, so agreement with CMB-based estimates that assume a flat ΛCDM cosmology is an important corroboration of this minimal cosmological model. For constant dark energy (Λ), our BAO+SN+CMB combination yields matter density $\Omega_m = 0.301 \pm 0.008$ and curvature $\Omega_k = -0.003 \pm 0.003$. When we allow more general forms of evolving dark energy, the BAO+SN+CMB parameter constraints are always consistent with flat ΛCDM values at $\approx 1\sigma$. While the overall χ^2 of model fits is satisfactory, the LyaF BAO measurements are in moderate $(2-2.5\sigma)$ tension with model predictions. Models with early dark energy that tracks the dominant energy component at high redshift remain consistent with our expansion history constraints, and they yield a higher H_0 and lower matter clustering amplitude, improving agreement with some low redshift observations. Expansion history alone yields an upper limit on the summed mass of neutrino species, $\sum m_\nu < 0.56\,\mathrm{eV}$ (95% confidence), improving to $\sum m_\nu < 0.25\,\mathrm{eV}$ if we include the lensing signal in the Planck CMB power spectrum. In a flat ΛCDM model that allows extra relativistic species, our data combination yields $N_{\rm eff} = 3.43 \pm 0.26$; while the LyaF BAO data prefer higher $N_{\rm eff}$ when excluding galaxy BAO, the galaxy BAO alone favor $N_{\rm eff} \approx 3$. When structure growth is extrapolated forward from the CMB to low redshift, standard dark energy models constrained by our data predict a level of matter clustering that is high compared to most, but not all, observational estimates.

Draft version September 24, 2014
Preprint typeset using LaTeX style emulateapj v. 05/12/14

Model independent evidence for dark energy evolution from baryon acoustic oscillations

V. Sahni[1], A. Shafieloo[2,3], A. A. Starobinsky[4,5]

Draft version September 24, 2014

ABSTRACT

Baryon Acoustic Oscillations (BAO) allow us to determine the expansion history of the Universe, thereby shedding light on the nature of dark energy. Recent observations of BAO's in the SDSS DR9 and DR11 have provided us with statistically independent measurements of $H(z)$ at redshifts of 0.57 and 2.34, respectively. We show that these measurements can be used to test the cosmological constant hypothesis in a model independent manner by means of an improved version of the Om diagnostic. Our results indicate that the SDSS DR11 measurement of $H(z) = 222 \pm 7$ km/sec/Mpc at $z = 2.34$, when taken in tandem with measurements of $H(z)$ at lower redshifts, imply considerable tension with the standard ΛCDM model. Our estimation of the new diagnostic Omh^2 from SDSS DR9 and DR11 data, namely $Omh^2 \approx 0.122 \pm 0.01$, which is equivalent to $\Omega_{0m}h^2 \approx 0.122 \pm 0.01$, which is equivalent to $\Omega_{0m}h^2$ for the spatially flat ΛCDM model, is in tension with the value $\Omega_{0m}h^2 = 0.1426 \pm 0.0025$ determined for ΛCDM from Planck+WP. This tension is alleviated in models in which the cosmological constant was dynamically *screened* (compensated) in the past. Such evolving dark energy models display a pole in the effective equation of state of dark energy at high redshifts, which emerges as a *smoking gun* test for these theories.

Subject headings: expansion history — cosmology: observations — methods: statistical

1. INTRODUCTION

There is ample observational evidence to suggest that the expansion of the universe is accelerating, fuelled perhaps by *dark energy* (DE) which violates the strong energy condition, so that $\rho + 3P < 0$. While the cosmological constant with $8\pi G T_{ik} = \Lambda g_{ik}$ and $P = -\rho \equiv -\Lambda/8\pi G$, envisioned by Einstein almost a century ago, fulfills this requirement, the tiny value associated with Λ has prompted theorists to look for alternatives in which dark energy evolves with time including modified gravity (Sahni & Starobinsky 2000; Carroll 2001; Peebles & Ratra 2003; Padmanabhan 2003; Sahni 2004; Copeland et al. 2006; Sahni & Starobinsky 2006; Clifton et al. 2012; Shafieloo 2014).

Meanwhile, the very simplicity of the cosmological constant has prompted the search for *null-diagnostics* which can inform us, on the basis of observations, whether or not DE is the cosmological constant.

One such diagnostic is the *Statefinder* $r = \dddot{a}/aH^3$ (also called the jerk) whose value stays pegged to unity *only in* ΛCDM (Sahni et al. 2003; Alam et al. 2003) (also

A second null diagnostic, $Om(z)$, is defined as (Sahni et al. 2008; Zunkel & Clarkson 2008)

$$Om(z) = \frac{\bar{h}^2(z) - 1}{(1+z)^3 - 1}\,, \quad \bar{h} = H(z)/H_0\,. \qquad (1)$$

A remarkable feature of Om is that its value remains pegged to Ω_{0m} in ΛCDM. In all other DE models the value of $Om(z)$ *evolves with time.*

While the Statefinder has proved exceedingly versatile in differentiating between rival DE models, a distinguishing feature of Om is that it depends only upon the expansion rate, $H(z)$, and is therefore easier to determine from observations than r (also see (Shafieloo et al. 2012; Visser 2004; Chiba & Nakamura 2000; Arabsalmani & Sahni 2011)). Om can also be written as a two-point diagnostic (Shafieloo et al. 2012)

$$Om(z_i; z_j) = \frac{\bar{h}^2(z_i) - \bar{h}^2(z_j)}{(1+z_i)^3 - (1+z_j)^3}, \qquad (2)$$

with $Om(z;0)$ defined in (1). Consequently, if the Hub-

Dynamical dark energy in light of the latest observations

Gong-Bo Zhao[1,2], Marco Raveri[3,4], Levon Pogosian[5,2], Yuting Wang[1,2], Robert G. Crittenden[2], Will J. Handley[6,7], Will J. Percival[2], Florian Beutler[2], Jonathan Brinkmann[8], Chia-Hsun Chuang[9,10], Antonio J. Cuesta[11,12], Daniel J. Eisenstein[13], Francisco-Shu Kitaura[14,15], Kazuya Koyama[2], Benjamin L'Huillier[16], Robert C. Nichol[2], Matthew M. Pieri[17], Sergio Rodriguez-Torres[9,18,19], Ashley J. Ross[20,2], Graziano Rossi[21], Ariel G. Sánchez[22], Arman Shafieloo[16,23], Jeremy L. Tinker[24], Rita Tojeiro[25], Jose A. Vazquez[26] & Hanyu Zhang[1]

A flat Friedman-Roberson-Walker universe dominated by a cosmological constant (Λ) and cold dark matter (CDM) has been the working model preferred by cosmologists since the discovery of cosmic acceleration[1,2]. However, tensions of various degrees of significance are known to be present among existing datasets within the ΛCDM framework[3–11]. In particular, the Lyman-α forest measurement of the Baryon Acoustic Oscillations (BAO) by the Baryon Oscillation Spectroscopic Survey (BOSS)[3] prefers a smaller value of the matter density fraction $\Omega_{\rm M}$ compared to the value preferred by cosmic microwave background (CMB). Also, the recently measured value of the Hubble constant, $H_0 = 73.24 \pm 1.74\,\mathrm{km\,s^{-1}\,Mpc^{-1}}$[12], is 3.4σ higher than $66.93 \pm 0.62\,\mathrm{km\,s^{-1}\,Mpc^{-1}}$ inferred from the Planck CMB data[7]. In this work, we investigate if these tensions can be interpreted as evidence for a non-constant dynamical dark energy (DE). Using the Kullback-Leibler (KL) divergence[13] to quantify the tension between

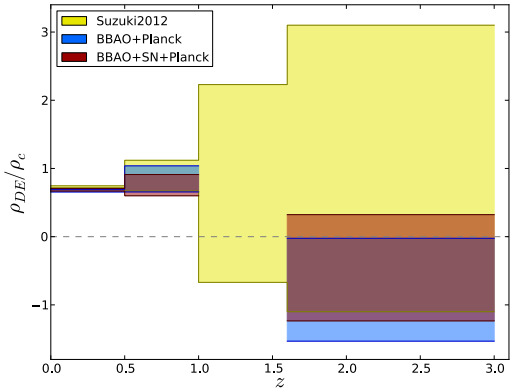

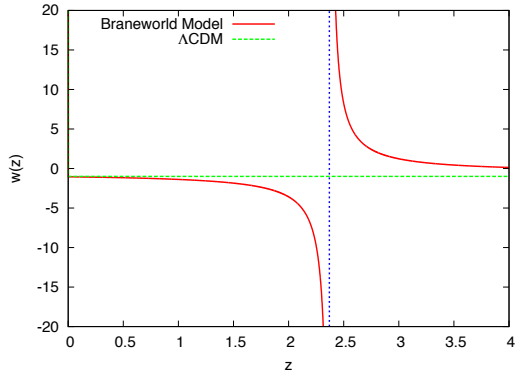

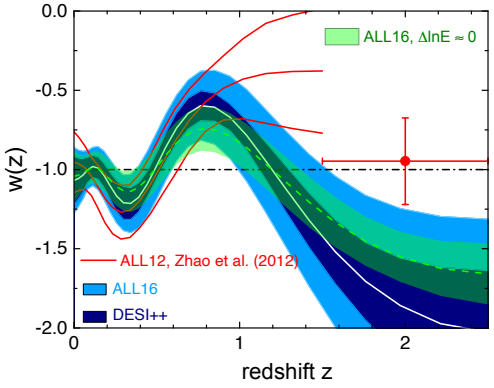

Sign-switching Λ - Λ_sCDM

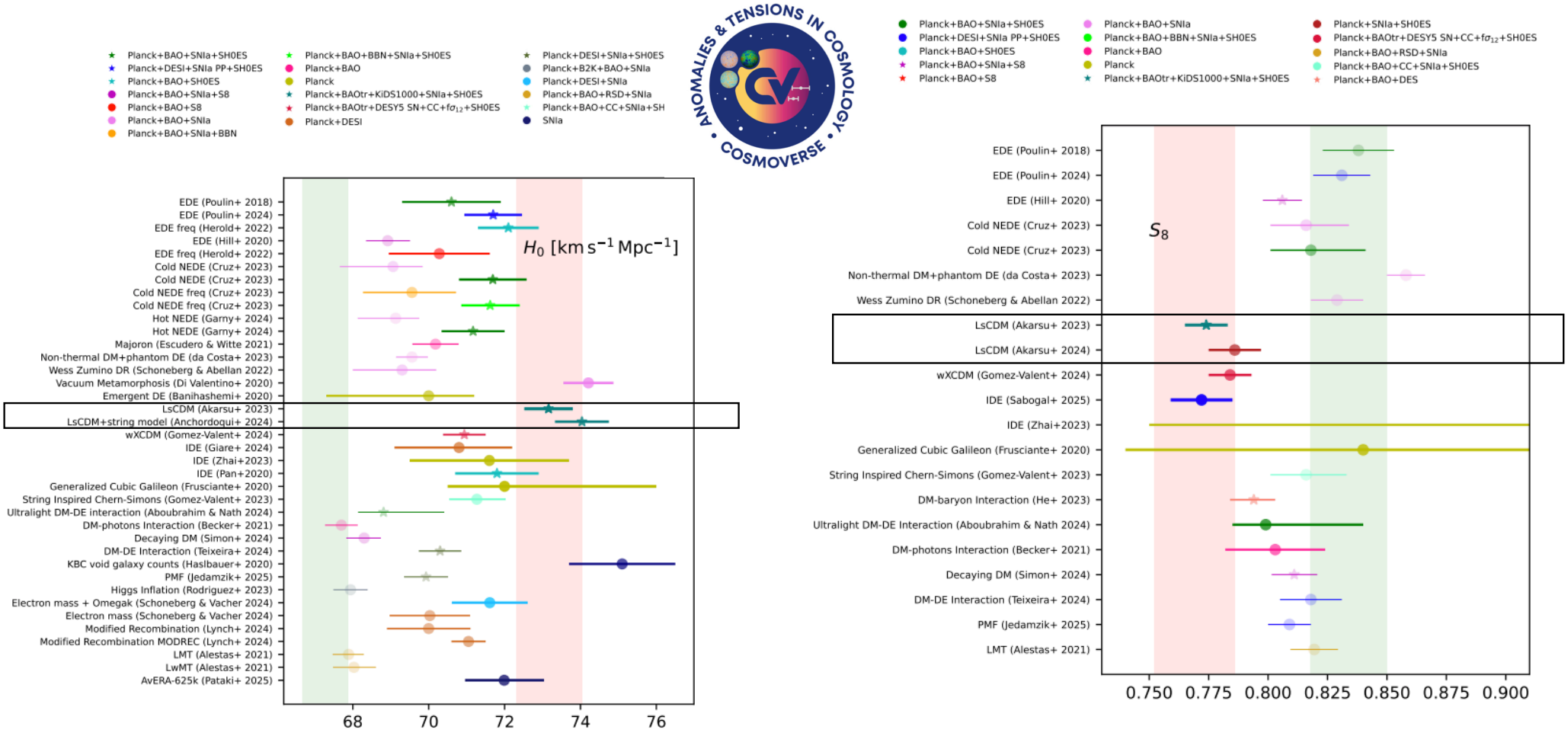

FIG. 3: Summary of models proposed to solve the H_0 tension in this White Paper following the order of the different sections.

FIG. 5: Summary of models proposed to solve the S_8 tension in this White Paper following the order of the different sections.

THE COSMOVERSE WHITE PAPER: ADDRESSING OBSERVATIONAL TENSIONS IN COSMOLOGY WITH SYSTEMATICS AND FUNDAMENTAL PHYSICS, DI VALENTINO, LEVI SAID, RIESS, POLLO ET AL. PHYS. DARK UNIV. 49 (2025) 101965 2504.01669

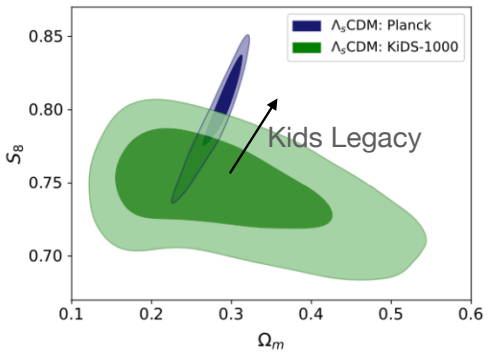

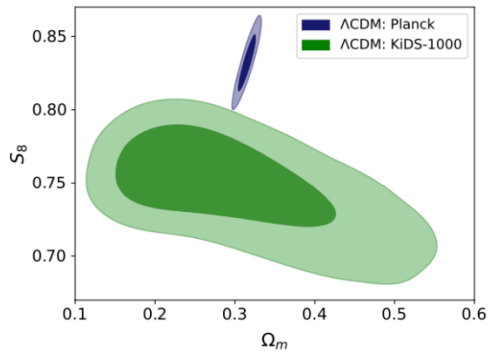

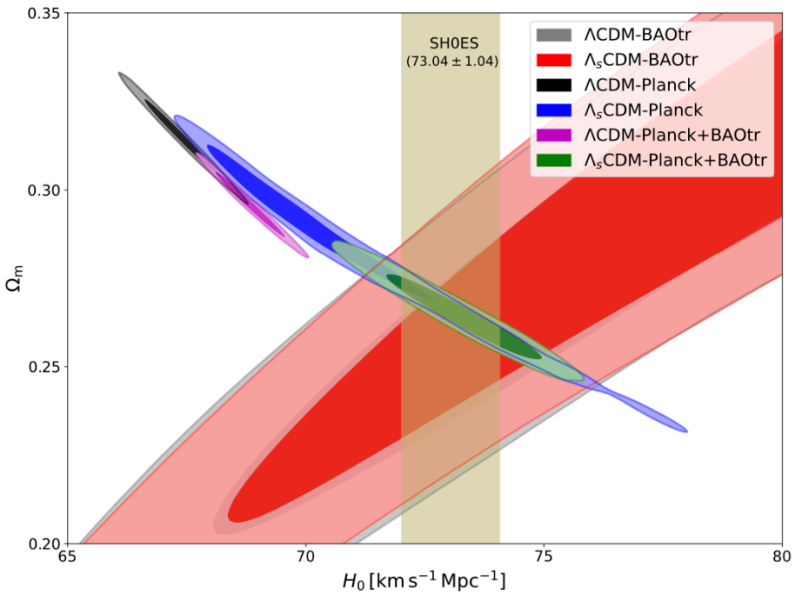

SH0ES 2024 L.Breuval et al. 2404.08038 [astro-ph.CO]].

$H_0 = 73.17 \pm 0.86$ km s^{-1} Mpc^{-1}

IT HAS CAPABILITY TO SIMULTANEOUSLY RESOLVE THE MAJOR COSMOLOGICAL TENSIONS, NOTABLY, H0, S8 AND MB TENSIONS ALONG WITH LESS SIGNIFICANT TENSIONS CURRENTLY PRESENT IN ΛCDM.

AKARSU, DI VALENTINO, KUMAR, NUNES, VAZQUEZ, YADAV, 2307.10899

Dataset	Planck	Planck+BAOtr	Planck+BAOtr+PP	Planck+BAOtr+PP&SH0ES	Planck+BAOtr+PP&SH0ES+KiDS-1000
Model	Λ_sCDM	Λ_sCDM	Λ_sCDM	Λ_sCDM	Λ_sCDM
	ΛCDM	ΛCDM	ΛCDM	ΛCDM	ΛCDM
$z_\dagger$	unconstrained	$1.70^{+0.09}_{-0.19}(1.65)$	$1.87^{+0.13}_{-0.21}(1.75)$	$1.70^{+0.10}_{-0.13}(1.67)$	$1.72^{+0.09}_{-0.12}(1.70)$
M_B[mag]	−−	−−	$-19.317^{+0.021}_{-0.025}(-19.311)$	$-19.290 \pm 0.017(-19.278)$	$-19.282 \pm 0.017(-19.280)$
	−−	−−	$-19.407 \pm 0.013(-19.411)$	$-19.379 \pm 0.012(-19.373)$	$-19.372 \pm 0.011(-19.369)$
H_0[km/s/Mpc]	$70.77^{+0.79}_{-2.70}(71.22)$	$73.30^{+1.20}_{-1.00}(73.59)$	$71.72^{+0.73}_{-0.92}(71.97)$	$72.82 \pm 0.65(73.20)$	$73.16 \pm 0.64(73.36)$
	$67.39 \pm 0.55(67.28)$	$68.84 \pm 0.48(68.61)$	$68.55 \pm 0.44(68.54)$	$69.57 \pm 0.42(69.73)$	$69.83 \pm 0.37(69.96)$
Ω_m	$0.2860^{+0.0230}_{-0.0099}(0.2796)$	$0.2643^{+0.0072}_{-0.0090}(0.2618)$	$0.2768^{+0.0072}_{-0.0063}(0.2759)$	$0.2683 \pm 0.0052(0.2646)$	$0.2646 \pm 0.0052(0.2622)$
	$0.3151 \pm 0.0075(0.3163)$	$0.2958 \pm 0.0061(0.2984)$	$0.2995 \pm 0.0056(0.2992)$	$0.2869 \pm 0.0051(0.2849)$	$0.2837 \pm 0.0045(0.2816)$
S_8	$0.801^{+0.026}_{-0.016}(0.791)$	$0.777 \pm 0.011(0.772)$	$0.791 \pm 0.011(0.794)$	$0.783 \pm 0.010(0.777)$	$0.774 \pm 0.009(0.773)$
	$0.832 \pm 0.013(0.835)$	$0.802 \pm 0.011(0.804)$	$0.808 \pm 0.010(0.804)$	$0.788 \pm 0.010(0.784)$	$0.781 \pm 0.008(0.782)$
$\Delta\chi^2_{\rm min}$	−2.46	−26.92	−15.50	−40.94	−41.16
$\ln\mathcal{B}_{ij}$	−1.28	−12.65	−7.52	−19.47	−19.77

Matching with SH0ES 2024 and H0DN 2026

- GROWTH TENSION AS WELL SPECIFICALLY, WHEN TREATING γ AS A FREE PARAMETER WITHIN ΛCDM FRAMEWORK, A COMBINATION OF PLANCK AND $f\sigma_8$ DATA YIELDS $\gamma \approx 0.64$, IN $\sim 4\sigma$ TENSION WITH THE THEORETICALLY EXPECTED VALUE $\gamma \approx 0.55$ (ASSUMING GR). [ESCAMILLA, AKARSU, DI VALENTINO, ÖZÜLKER & VAZQUEZ, 2503.12945]

NYUGEN ET AL. 2302.01331

Λ_sCDM turns "negative neutrino mass" into physical neutrino mass

recovers *physical* neutrino masses — not just a better fit

Kibris, Elbers, Akarsu & Di Valentino, "Negative neutrino mass or negative dark energy?" arXiv:2605.21456

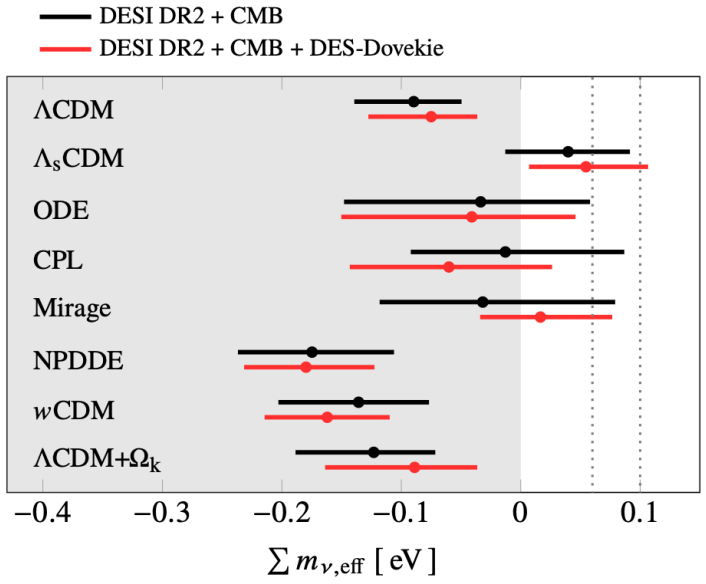

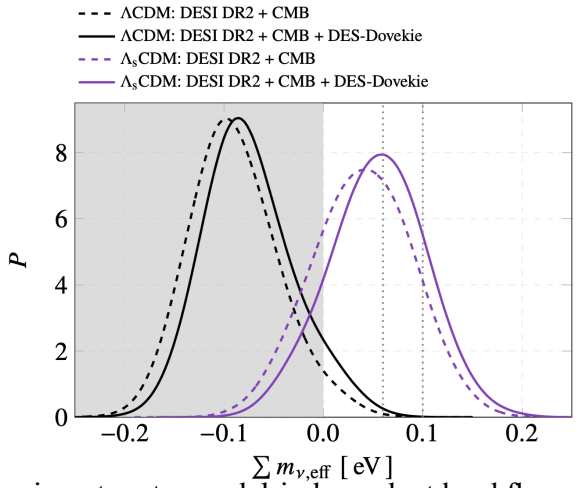

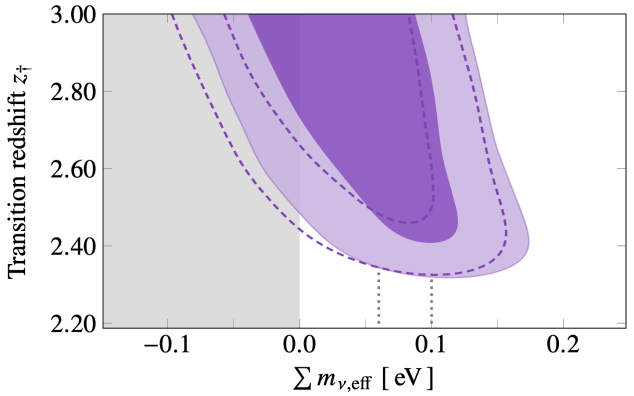

FIG. 4. Summary of the constraints on the effective neutrino mass parameter, $\sum m_{\nu,\mathrm{eff}}$, from DESI DR2 BAO + CMB alone (black) and combined with DES-Dovekie SNe (red), for the set of models considered in this work. Points and horizontal bars indicate marginalized posterior means and 68% credible intervals. The vertical dotted lines denote the lower bounds from neutrino oscillation experiments for the normal and inverted orderings. The figure highlights that Λ_sCDM is the only model in the current set that yields a 68% credible interval for $\sum m_{\nu,\mathrm{eff}}$ entirely within the positive range for the full data combination.

Oscillation experiments set a model-independent hard floor:
$\Sigma m_\nu \geq 0.059$ eV. Any cosmology that prefers a negative mass conflicts not just with another dataset, but with established particle physics.

Within ΛCDM, DESI + CMB push the inferred mass into the *unphysical* negative region ($\Sigma m_{\nu,\mathrm{eff}} = -0.075$ eV).

ΛsCDM is the only model in the set that returns a *physical, positive* value ($\Sigma m_{\nu,\mathrm{eff}} = +0.055 \pm 0.050$ eV), with its with the oscillation lower bound.

ΛsCDM is *not* the best-fitting model: several dark-energy models lower χ^2 more, and Bayesian evidence penalizes the extra parameters — yet they all leave the neutrino mass negative.
A lower χ^2 with unphysical parameters is no resolution at all;
ΛsCDM's distinction is physical consistency, not statistical superiority.

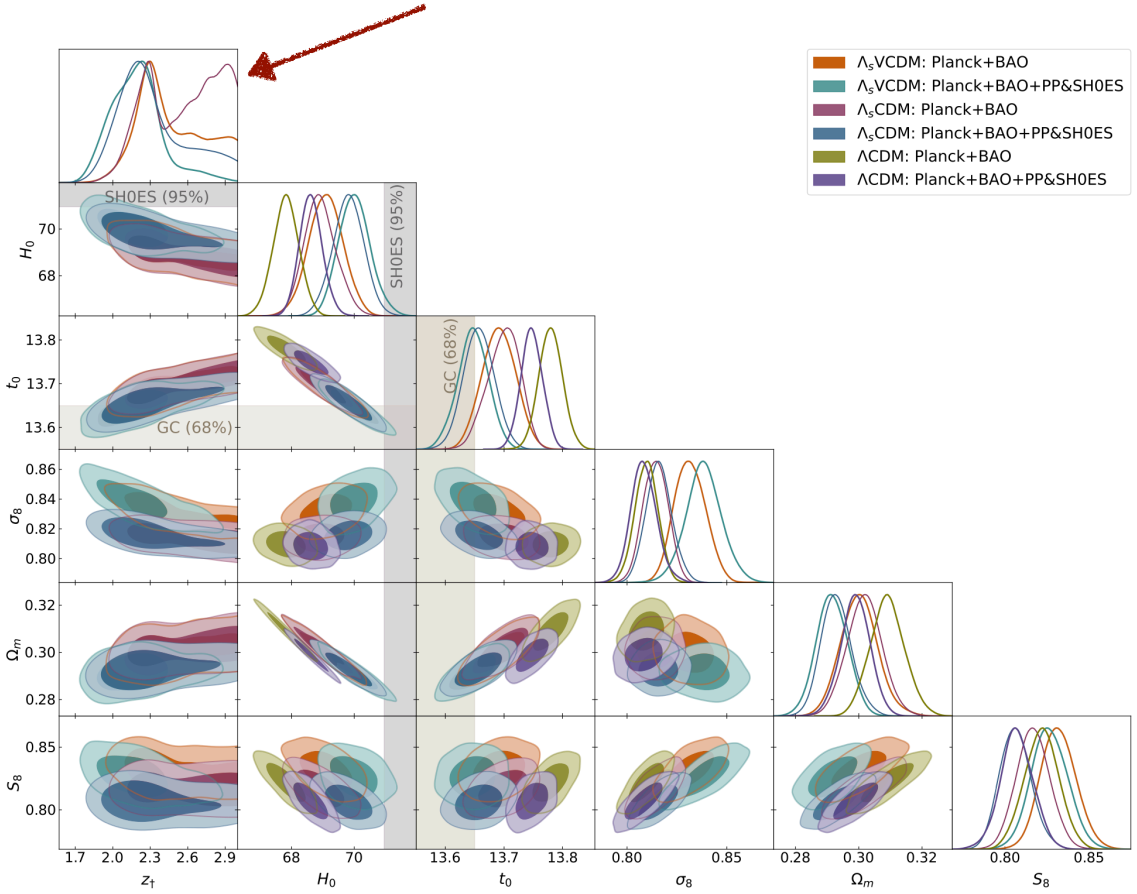

FIG. 3. One- and two-dimensional (68% and 95% CL) marginalized distributions of the Λ_sVCDM, Λ_sCDM, and ΛCDM model parameters from Planck+BAO and Planck+BAO+PP&SH0ES. The vertical violet and brown bands show the local measurements of $H_0 = 73.04 \pm 1.04$ km s^{-1} Mpc^{-1} (SH0ES) [10] and $t_0 = 13.50 \pm 0.15$ Gyr (stat.) [99].

TABLE II. Marginalized constraints (mean values with 68% CL limits) for the free and selected derived parameters of the Λ_sCDM, Λ_sVCDM, and ΛCDM models across different dataset combinations. The relative best fit $\Delta\chi^2_{\rm min}$, Akaike information criterion ΔAIC, and log-Bayesian evidence $\Delta \ln \mathcal{Z}$ are also provided; negative values indicate a preference for the Λ_sCDM/Λ_sVCDM models over the standard ΛCDM model.

Dataset	Planck	Planck+BAO(z>0.8)	Planck+BAO	Planck +PP&SH0ES	Planck+BAO(z>0.8) +PP&SH0ES	Planck+BAO +PP&SH0ES
Model	**Λ_sCDM**	**Λ_sCDM**	**Λ_sCDM**	**Λ_sCDM**	**Λ_sCDM**	**Λ_sCDM**
	Λ_sVCDM	**Λ_sVCDM**	**Λ_sVCDM**	**Λ_sVCDM**	**Λ_sVCDM**	**Λ_sVCDM**
	ΛCDM	**ΛCDM**	**ΛCDM**	**ΛCDM**	**ΛCDM**	**ΛCDM**
$10^2\omega_b$	2.241 ± 0.015	2.243 ± 0.015	2.237 ± 0.014	2.246 ± 0.015	$2.245^{+0.015}_{-0.013}$	$2.245^{+0.015}_{-0.013}$
	2.250 ± 0.015	2.243 ± 0.015	2.236 ± 0.014	2.246 ± 0.015	2.249 ± 0.014	2.244 ± 0.014
	2.238 ± 0.014	2.245 ± 0.015	2.244 ± 0.014	2.264 ± 0.014	2.267 ± 0.014	2.262 ± 0.013
$\omega_{\rm cdm}$	0.1195 ± 0.0012	0.1193 ± 0.0011	0.1203 ± 0.0010	0.1190 ± 0.0010	0.1192 ± 0.0010	0.1197 ± 0.0010
	0.1185 ± 0.0013	$0.1191^{+0.0012}_{-0.0011}$	0.1203 ± 0.0010	0.1190 ± 0.0011	0.1191 ± 0.0011	0.1198 ± 0.0010
	0.1200 ± 0.0012	0.1189 ± 0.0011	0.1191 ± 0.0009	0.1173 ± 0.0010	0.1168 ± 0.0010	0.1175 ± 0.0008
$100\theta_s$	1.04189 ± 0.00029	1.04192 ± 0.00029	1.04185 ± 0.00028	1.04194 ± 0.00029	1.04198 ± 0.00028	1.04195 ± 0.00029
	1.04201 ± 0.00030	1.04194 ± 0.00030	1.04184 ± 0.00029	$1.04197^{+0.00028}_{-0.00032}$	1.04198 ± 0.00029	1.04190 ± 0.00030
	$1.04190^{+0.00027}_{-0.00031}$	1.04198 ± 0.00029	1.04198 ± 0.00028	1.04217 ± 0.00028	1.04223 ± 0.00028	1.04216 ± 0.00028
$\ln(10^{10}A_s)$	3.040 ± 0.014	$3.041^{+0.011}_{-0.015}$	3.037 ± 0.014	$3.039^{+0.012}_{-0.014}$	$3.039^{+0.013}_{-0.015}$	$3.040^{+0.012}_{-0.014}$
	3.033 ± 0.016	3.036 ± 0.015	3.034 ± 0.014	3.032 ± 0.015	3.034 ± 0.015	3.036 ± 0.014
	3.046 ± 0.014	$3.049^{+0.013}_{-0.015}$	3.048 ± 0.014	$3.058^{+0.015}_{-0.017}$	3.059 ± 0.015	$3.056^{+0.014}_{-0.016}$
n_s	0.9669 ± 0.0043	0.9672 ± 0.0040	0.9645 ± 0.0039	0.9684 ± 0.0039	0.9676 ± 0.0038	0.9663 ± 0.0040
	0.9694 ± 0.0044	0.9678 ± 0.0041	0.9646 ± 0.0035	0.9677 ± 0.0039	0.9677 ± 0.0038	0.9660 ± 0.0038
	0.9657 ± 0.0041	0.9681 ± 0.0039	0.9675 ± 0.0036	0.9722 ± 0.0039	$0.9736^{+0.0036}_{-0.0041}$	0.9720 ± 0.0036
$\tau_{\rm reio}$	0.0528 ± 0.0073	$0.0536^{+0.0059}_{-0.0078}$	0.0509 ± 0.0072	$0.0530^{+0.0060}_{-0.0074}$	$0.0528^{+0.0055}_{-0.0076}$	$0.0527^{+0.0057}_{-0.0071}$
	0.0507 ± 0.0076	0.0514 ± 0.0076	0.0493 ± 0.0071	$0.0498^{+0.0078}_{-0.0069}$	$0.0504^{+0.0079}_{-0.0070}$	0.0504 ± 0.0074
	0.0550 ± 0.0072	$0.0573^{+0.0065}_{-0.0082}$	$0.0568^{+0.0066}_{-0.0074}$	$0.0630^{+0.0073}_{-0.0087}$	0.0642 ± 0.0079	$0.0620^{+0.0067}_{-0.0084}$
$z_\dagger$	> 1.45 (95% CL)	$2.20^{+0.17}_{-0.38}$	> 2.11 (95% CL)	$1.83^{+0.11}_{-0.19}$	$1.87^{+0.11}_{-0.18}$	$2.31^{+0.15}_{-0.36}$
	$1.88^{+0.28}_{-0.58}$ [> 1.20 (95% CL)]	$2.12^{+0.23}_{-0.27}$	> 2.06 (95% CL)	$1.80^{+0.13}_{-0.18}$	$1.86^{+0.12}_{-0.21}$	$2.20^{+0.16}_{-0.23}$
	-	-	-	-	-	-
H_0[km/s/Mpc]	$70.77^{+0.79}_{-2.70}$	$70.39^{+0.87}_{-1.20}$	$68.92^{+0.46}_{-0.55}$	72.07 ± 0.88	71.68 ± 0.73	69.82 ± 0.49
	$73.40^{+1.80}_{-1.60}$	$70.72^{+0.87}_{-1.30}$	69.10 ± 0.55	72.25 ± 0.91	71.86 ± 0.79	70.01 ± 0.50
	67.39 ± 0.55	67.88 ± 0.51	67.82 ± 0.41	68.69 ± 0.47	68.91 ± 0.46	$68.62^{+0.34}_{-0.38}$
Ω_m	$0.2860^{+0.0230}_{-0.0099}$	$0.2880^{+0.0100}_{-0.0088}$	0.3018 ± 0.0056	0.2738 ± 0.0072	0.2770 ± 0.0063	$0.2929^{+0.0044}_{-0.0051}$
	$0.2650^{+0.0340}_{-0.0190}$	$0.2850^{+0.0110}_{-0.0091}$	0.3001 ± 0.0059	0.2725 ± 0.0073	0.2755 ± 0.0065	0.2915 ± 0.0049
	0.3151 ± 0.0075	0.3083 ± 0.0067	0.3091 ± 0.0054	0.2981 ± 0.0060	0.2952 ± 0.0058	0.2989 ± 0.0046
σ_8	$0.8210^{+0.0064}_{-0.0110}$	$0.8169^{+0.0062}_{-0.0070}$	0.8143 ± 0.0062	0.8228 ± 0.0068	0.8215 ± 0.0067	0.8160 ± 0.0065
	$0.8620^{+0.0160}_{-0.0380}$	$0.8414^{+0.0094}_{-0.0140}$	0.8316 ± 0.0078	0.8560 ± 0.0120	0.8520 ± 0.0110	0.8385 ± 0.0090
	$0.8121^{+0.0055}_{-0.0061}$	0.8098 ± 0.0061	0.8097 ± 0.0058	$0.8085^{+0.0060}_{-0.0070}$	0.8077 ± 0.0062	$0.8085^{+0.0060}_{-0.0067}$
S_8	$0.801^{+0.026}_{-0.016}$	0.800 ± 0.014	0.817 ± 0.010	0.786 ± 0.011	0.789 ± 0.010	$0.806^{+0.009}_{-0.010}$
	$0.808^{+0.021}_{-0.017}$	0.819 ± 0.012	0.832 ± 0.011	0.815 ± 0.011	$0.816^{+0.011}_{-0.012}$	0.826 ± 0.011
	0.832 ± 0.013	0.821 ± 0.012	0.822 ± 0.010	0.806 ± 0.011	0.801 ± 0.011	0.807 ± 0.010
t_0[Gyr]	$13.62^{+0.12}_{-0.04}$	$13.64^{+0.05}_{-0.04}$	$13.70^{+0.03}_{-0.02}$	13.56 ± 0.04	13.58 ± 0.03	13.66 ± 0.03
	$13.52^{+0.18}_{-0.09}$	$13.62^{+0.06}_{-0.04}$	13.69 ± 0.03	13.56 ± 0.04	13.57 ± 0.04	13.65 ± 0.03
	13.79 ± 0.02	13.78 ± 0.02	13.78 ± 0.02	13.75 ± 0.02	13.74 ± 0.02	13.75 ± 0.02
$\chi^2_{\rm min}$	2778.06	2785.48	2796.16	4082.28	4086.42	4106.24
	2777.36	2782.92	2793.42	4079.60	4086.34	4106.30
	2780.52	2792.14	2797.44	4105.80	4114.24	4122.20
$\Delta\chi^2_{\rm min}$	-2.46	-6.66	-1.28	-23.52	-27.82	-15.96
	-3.16	-9.22	-4.02	-26.20	-27.90	-15.90
ΔAIC	-0.46	-4.66	0.72	-21.52	-25.82	-13.96
	-1.16	-7.22	-2.02	-24.20	-25.90	-13.90
$\ln \mathcal{Z}$	-1423.17	-1427.41	-1432.97	-2076.65	-2079.93	-2089.64
	-1422.21	-1425.95	-1432.39	-2074.32	-2078.44	-2088.24
	-1424.45	-1429.64	-1433.52	-2088.18	-2092.07	-2096.01
$\Delta \ln \mathcal{Z}$	-1.28	-2.23	-0.55	-11.53	-12.14	-6.37
	-2.24	-3.69	-1.13	-13.86	-13.63	-7.77

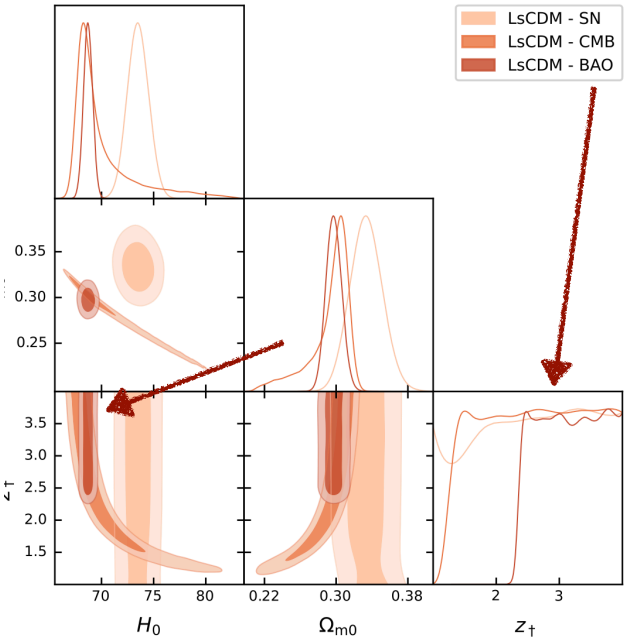

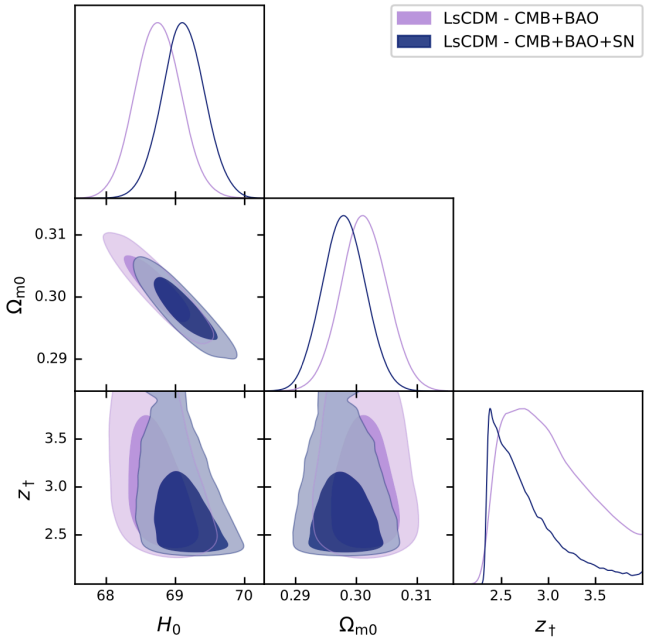

(A) Abrupt Λ_sCDM

Model	χ^2	ΔAIC	ΔAIC$_c$	ΔBIC
		CMB+BAO+SN		
ΛCDM	1500.370	0.000	0.000	0.000
Λ_sCDM	1489.347	-9.023	-9.014	-3.574
LΛCDM	1487.836	-8.535	-8.514	2.363
SSCDM	1488.956	-7.414	-7.393	3.484
ECDM	1488.917	-7.553	-7.532	3.344

"Sign-Switching Dark Energy: Smooth Transitions with Recent DESI DR2 Observations"
Ibarra-Uriondo & Bouhmadi-López, Physics of the Dark Universe, arXiv:2602.12347

GENUINE THEORETICAL EMBEDDING FOR Λ_sCDM

Can they be distinguishable from different predictions from ΛCDM and from each others?

✓ Overall sign change of the metric: imaginary space extensions of the usual Lorentzian theory, with $a^2 < 0$ [alexandre, gielen, magueijo, JCAP 02 (2024) 036, 230611502]

$$\tilde{\Lambda} = \mathrm{sgn}(\tilde{a}^2)\Lambda$$

✓ a string inspired model where Casimir forces of fields inhabiting the bulk of the dark dimension scenario [Anchordoqui & antoniadis & lüst, Phys. Lett. B 855 (2024) 138775, 2312.12352, Anchordoqui, antoniadis, lüst, noble & soriano, Phys. Dark Univ. 46 (2024) 101715 2404.17334]

✓ Type II minimally modified gravity (VCDM) [Akarsu De felice, di Valentino, kumar, nunes, özülker, vazquez, yadav, MNRAS 546 (2026) 1 2402.07716 & PRD 110, 103527 (2024) 2406.07526]

$$\tilde{\rho}_{\mathrm{eff}} = \frac{1}{\tilde{\kappa}}\left[\tilde{\kappa}\tilde{\rho} - \frac{n(n-1)}{2}\frac{\dot{s}^2}{s^2} - n\frac{\dot{s}}{s}\left(\frac{\dot{a}}{a} + \frac{\dot{b}}{b} + \frac{\dot{c}}{c}\right)\right],$$

✓ The former negative correlation between the spaces, along with the accelerated expansion of the external space, such as a wormhole-type continuation, may reverse the correlation from negative to positive. $\lambda < 0 \to \lambda > 0$ causing both spaces to begin expanding. katirci, JHeap 45 382 (2025) , 2501.02109

✓ Unexplored regions in teleparallel f(T) gravity: Sign-changing dark energy density [Akarsu, Bulduk, De Felice, katirci, Uzun, PRD 112, 083532 (2025) 2410.23068] (Torsion or Non-metricity)

✓ Construction of Λ_sCDM from spatial curvature of internal space [akarsu, bulduk, katirci, özülker, Perivolaropoulos] ongoing work

by embedding ΛCDM in a (1 + 3 + n)-dimensional Kaluza–Klein spacetime with compact extra dimensions of constant intrinsic curvature

$$\Lambda_s = \Lambda_{s0}\frac{n(n-1)}{4}k_{\mathrm{int}}\left(\frac{1}{s_{\mathrm{p}}^2} - \frac{1}{s_0^2}\right)$$

$$G_{4\mathrm{Dp}} = G_{4\mathrm{D0}}\left(\frac{s_{\mathrm{p}}}{s_0}\right)^{-n}$$

A Geometric Route to Λ_SCDM from Curved Internal space

Beginning with Curvature-induced sign transitions in four dimensions

$$z_{o\Lambda\dagger} = -1 + \sqrt{-\frac{\Omega_\Lambda}{\Omega_{k0}}},$$

Simple-graduated dark energy and spatial curvature, Acquaviva, Akarsu, Katirci and Vazquez, Phys. Rev. D **104** (2021), 023505 2104.02623

Dark Energy with Constant Inertial Mass Density: Updated Constraints and Curvature-Induced Sign Transitions in ρ_{DE} and $\rho_{DE} + p_{DE}$,

Escamilla, Karadavut & Katirci, 2603.15868

$$\Omega_{k0} < 0$$

Di Valentino, Melchiorri, Silk, Nature Astron. 1911.02087, 2003.04935 , Handley, 1908.09139

Dataset	BAO+CC+SN+SH0ES		
	oΛCDM	owCDM	osimple-gDE
Ω_{m0}	0.301 ± 0.011	0.309 ± 0.011	0.313 ± 0.011
$\Omega_{b0}h_0^2$	0.0224 ± 0.0004	0.0224 ± 0.0004	0.0224 ± 0.0004
h_0	0.698 ± 0.015	0.697 ± 0.015	0.717 ± 0.014
w_{kci0}	-1	-0.941 ± 0.047	-0.536 ± 0.228
Ω_{k0}	0.021 ± 0.036	-0.036 ± 0.041	-0.035 ± 0.026
$\varrho_{kci} \times 10^{31}$ [g cm^{-3}]	0	2.296 ± 3.091	$18.6^{+27.1}_{-29.9}$
Ω_{ci0}	0.639 ± 0.025	0.658 ± 0.037	0.641 ± 0.027
Ω_{kci0}	0.652 ± 0.011	0.649 ± 0.011	0.652 ± 0.010
$z_{kci\dagger}$ $(>0)(68\%)$	$6.21^{+5.41}_{-2.27}$	$4.49^{+4.25}_{-1.63}$	$1.51^{+0.68}_{-0.34}$ & $13.1^{+14.5}_{-6.6}$
χ^2_{min}	-1423.972	-1423.371	-1417.546
$\Delta\chi^2_{min}$	0	-0.60	-6.43
$\ln \mathcal{Z}$	-728.857	-730.511	-725.222
$\Delta \ln \mathcal{Z}$	0	1.65	-3.63

$$\Omega_{kci} = \Omega_{ci0}\left[1 + 3(1 + w_{ci0})\ln(1+z)\right] + \Omega_{k0}(1+z)^2,$$

$$w_{ci0} > -1,$$

$$z_{kci\dagger} = \begin{cases} -1 + e^{-\frac{1}{3(1+w_{ci0})} - \frac{1}{2}W_{-1}(x)}, \\ -1 + e^{-\frac{1}{3(1+w_{ci0})} - \frac{1}{2}W_{0}(x)}, \end{cases}$$

$$x = \frac{\Omega_{k0}}{\Omega_{ci0}} \frac{2}{3(1+w_{ci0})} e^{-\frac{2}{3(1+w_{ci0})}},$$

$$z_{kci\dagger} = -1 + e^{-\frac{1}{3(1+w_{ci0})} - \frac{1}{2}W_{0}(x)},$$

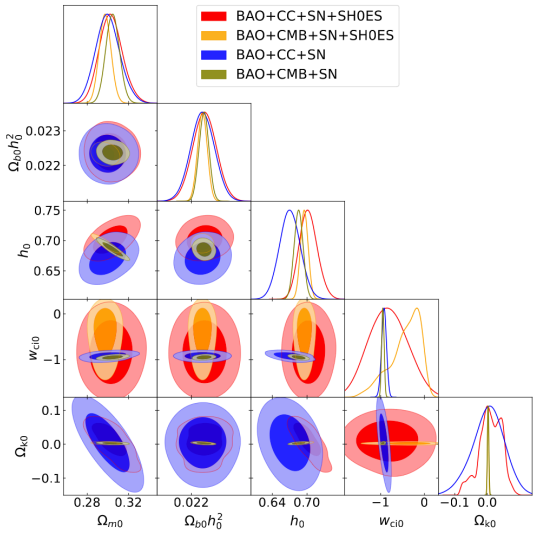

FIG. 8. One- and two-dimensional (68% and 95% CLs) marginalized posterior distributions for the free parameters of *o*SimpleGDE model using the combined datasets.

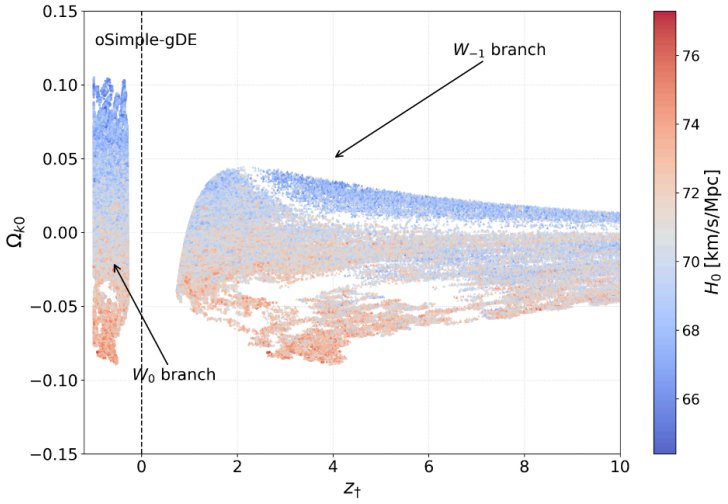

For the BAO+CC+SN+SH0ES dataset, the *o*Simple-gDE model yields a transition redshift $z^\dagger = 1.51^{+0.68}_{-0.34}$ in the W_{-1} branch, while the crossing of the Null Energy Condition boundary (NECB), defined by $\rho_{DE} + p_{DE} = 0$, occurs at $z_{NECB} = 2.36^{+1.48}_{-1.48}$.

INTERNAL DIMENSIONS?

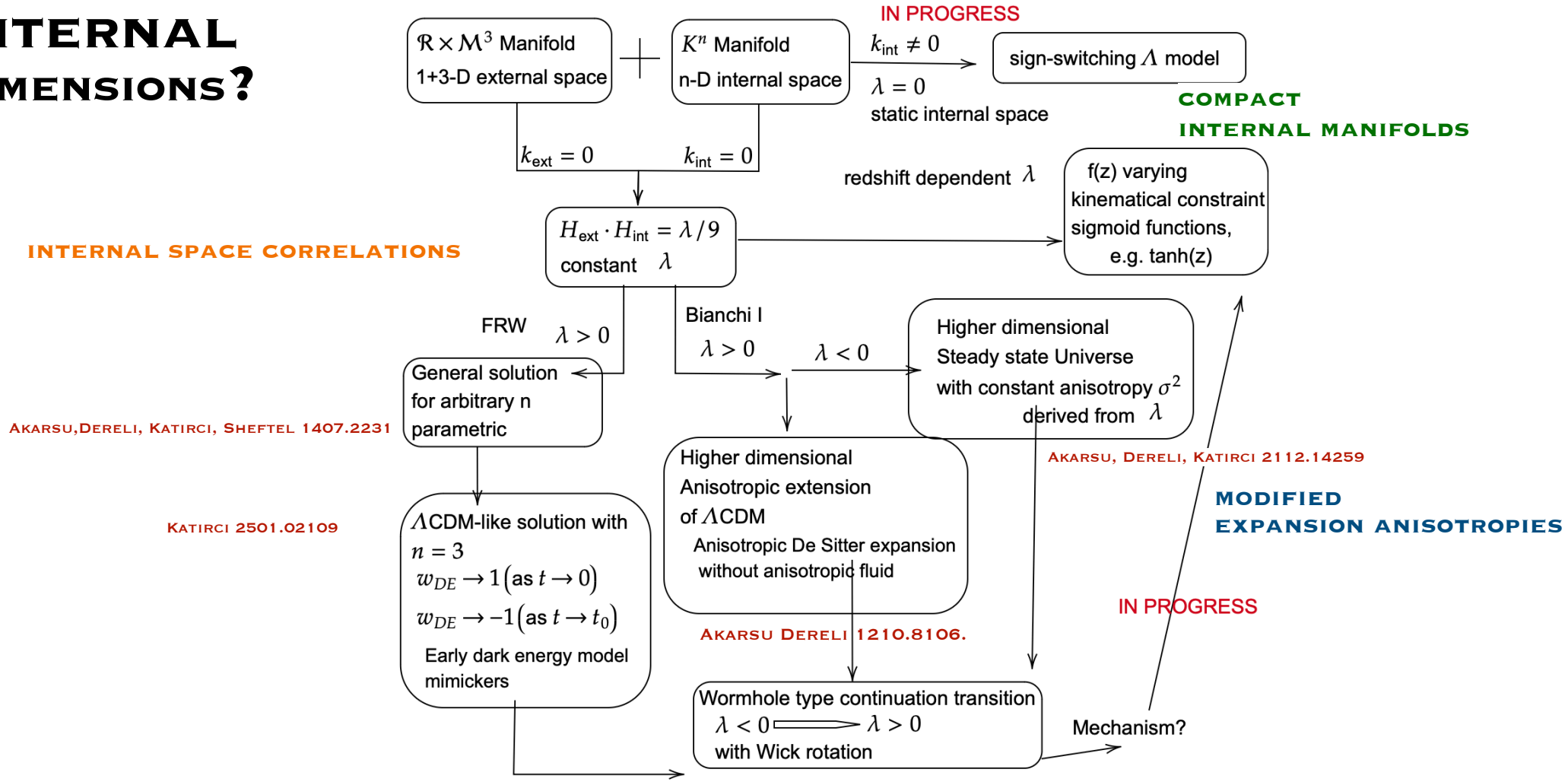

Taken from “Role of internal space correlations in the dynamics of a higher-dimensional Bianchi type-I universe: shear scalar and Hubble parameter perspectives”
KATIRCI, JOURNAL OF HIGH ENERGY ASTROPHYSICS 45 382 (2025) , 2501.02109

Constructing Λ_sCDM model from compact internal space manifold

$k_{\rm ext}=0$

Akarsu, Bulduk, Katirci, Özülker and Perivolaropoulos, ongoing work

Is internal space CURVED ?

$$\mathcal{M}^{1+3+n}=\mathcal{R}\times M^3\times\mathcal{K}^n,$$

$$\tilde{R}_{\mu\nu}-\frac{1}{2}\tilde{g}_{\mu\nu}\tilde{R}+\tilde{\Lambda}\tilde{g}_{\mu\nu}=\tilde{\kappa}\tilde{T}_{\mu\nu},$$

$$ds^2=-dt^2+a^2(t)\frac{d\vec{x}^{\,2}}{\left(1+k_{\rm ext}|\vec{x}|^2/4\right)^2}+s^2(t)\frac{d\vec{y}^{\,2}}{\left(1+k_{\rm int}|\vec{y}|^2/4\right)^2},$$

$$\tilde{T}_\mu{}^\nu=\mathrm{diag}[-\tilde{\rho},\tilde{p}_{\rm ext},\tilde{p}_{\rm ext},\tilde{p}_{\rm ext},\tilde{p}_{\rm int},\dots,\tilde{p}_{\rm int}],$$

Therefore, the scenario is observationally indistinguishable from ΛCDM model

$$\tilde{\gamma}\equiv\tilde{\Lambda}+\tilde{\chi}.$$

3 equations and 5 unknown

$$3\left[\frac{\dot{a}^2}{a^2}+\frac{k_{\rm ext}}{a^2}\right]+3n\frac{\dot{a}}{a}\frac{\dot{s}}{s}+\frac{1}{2}n(n-1)\left[\frac{\dot{s}^2}{s^2}+\frac{k_{\rm int}}{s^2}\right]-\tilde{\Lambda}=\tilde{\kappa}\tilde{\rho},$$

$$2\frac{\ddot{a}}{a}+\frac{\dot{a}^2}{a^2}+\frac{k_{\rm ext}}{a^2}+n\frac{\ddot{s}}{s}+2n\frac{\dot{a}}{a}\frac{\dot{s}}{s}+\frac{1}{2}n(n-1)\left[\frac{\dot{s}^2}{s^2}+\frac{k_{\rm int}}{s^2}\right]-\tilde{\Lambda}=-\tilde{\kappa}\tilde{p}_{\rm ext},\qquad(6)$$

$$3\left[\frac{\ddot{a}}{a}+\frac{\dot{a}^2}{a^2}+\frac{k_{\rm ext}}{a^2}\right]+(n-1)\left[\frac{\ddot{s}}{s}+3\frac{\dot{a}}{a}\frac{\dot{s}}{s}\right]+\frac{1}{2}(n-1)(n-2)\left[\frac{\dot{s}^2}{s^2}+\frac{k_{\rm int}}{s^2}\right]-\tilde{\Lambda}=-\tilde{\kappa}\tilde{p}_{\rm int}.$$

$$3\frac{\dot{a}^2}{a^2}+\frac{1}{2}n(n-1)\frac{k_{\rm int}}{s_*^2}-\tilde{\Lambda}=\tilde{\kappa}\tilde{\rho},$$

$$\frac{\dot{a}^2}{a^2}+2\frac{\ddot{a}}{a}+\frac{1}{2}n(n-1)\frac{k_{\rm int}}{s_*^2}-\tilde{\Lambda}=-\tilde{\kappa}\tilde{p}_{\rm ext},$$

$$3\frac{\dot{a}^2}{a^2}+3\frac{\ddot{a}}{a}+\frac{1}{2}(n-1)(n-2)\frac{k_{\rm int}}{s_*^2}-\tilde{\Lambda}=-\tilde{\kappa}\tilde{p}_{\rm int}.$$

$$\tilde{\chi}\equiv-\frac{n(n-1)}{2}\frac{k_{\rm int}}{s_*^2}.$$

$$H_{\rm ext}^2=\frac{\tilde{\kappa}\tilde{\rho}_{\rm m0}}{3}a^{-3}+\frac{\tilde{\gamma}}{3},$$

$$\tilde{w}_{\tilde{\chi}}=\left\{-1,-1,-1,-1+\frac{2}{n},-1+\frac{2}{n},\dots\right\},$$

$$\tilde{\gamma}>0\quad\rightarrow\quad\tilde{\Omega}_{\tilde{\gamma}}>0,$$

+1 equation

$$s=s_*=\text{const.},\qquad\tilde{w}_{\rm ext}=0$$

$$\rho_{\rm m}=\frac{\tilde{\kappa}}{\kappa}\tilde{\rho}_{\rm m}=s_*^n\tilde{\rho}_{\rm m}\quad\text{and}\quad p_{\rm m}=\frac{\tilde{\kappa}}{\kappa}\tilde{p}_{\rm ext}=0,$$

$$\dot{\tilde{\rho}}+\left(3\frac{\dot{a}}{a}+n\frac{\dot{s}}{s}\right)\tilde{\rho}+3\frac{\dot{a}}{a}\tilde{p}_{\rm ext}+n\frac{\dot{s}}{s}\tilde{p}_{\rm int}=0.$$

$$\dot{\tilde{\rho}}+3\frac{\dot{a}}{a}(1+\tilde{w}_{\rm ext})\tilde{\rho}=0,$$

+1 equation

$$\frac{\tilde{\kappa}}{\kappa}\propto s_*^n=V_{\rm int}=\text{const.},$$

Construction of Λ_sCDM model from compact internal space manifold

Akarsu, Bulduk, Katirci, Özülker and Perivolaropoulos, ongoing work

~~$s = s_* = \text{const.}$~~,

+1 equation

$$s(t) = s_{\rm p} + (s_0 - s_{\rm p})\theta\,(t - t_\dagger)\,,$$

$$\tilde{w}_{\rm ext} = 0$$

+1 equation

$$\theta(t-t_\dagger) = \begin{cases} 0, & t < t_\dagger, \\ 1, & t \geq t_\dagger, \end{cases}$$

$$s(t) = \begin{cases} s_{\rm p} & \text{for} \quad t < t_\dagger, \\ s_0 & \text{for} \quad t \geq t_\dagger. \end{cases}$$

$$a = \begin{cases} a_0 \left(\frac{1}{\alpha(1-\tilde{\Omega}_{\rm m0})} - 1\right)^{\frac{1}{3}} \sinh^{\frac{2}{3}}\left[\frac{3H_{\rm ext0}\sqrt{\alpha(1-\tilde{\Omega}_{\rm m0})}}{2}\, t\right] \\ a_0 \left(\frac{\tilde{\Omega}_{\rm m0}}{1-\tilde{\Omega}_{\rm m0}}\right)^{\frac{1}{3}} \sinh^{\frac{2}{3}}\left[\frac{3H_{\rm ext0}\sqrt{1-\tilde{\Omega}_{\rm m0}}}{2}(t-b)\right] \end{cases}$$

where

$$a_0 = \left(\frac{\tilde{\Omega}_{\rm m0}}{1-\tilde{\Omega}_{\rm m0}}\right)^{-1/3} \sinh^{-2/3}\left[\frac{3H_{\rm ext0}\sqrt{1-\tilde{\Omega}_{\rm m0}}}{2}(t_0 - b)\right],$$

$$b = t_\dagger - \frac{2\text{arcsinh}\left[\sqrt{\frac{1-\alpha(1-\tilde{\Omega}_{\rm m0})}{\alpha\tilde{\Omega}_{\rm m0}}}\sinh\left(\frac{3\mathrm{H}_{\rm ext0}\sqrt{1-\tilde{\Omega}_{\rm m0}}}{2}\mathrm{t}_\dagger\right)\right]}{3H_{\rm ext0}\sqrt{1-\tilde{\Omega}_{\rm m0}}}.$$

when the internal space undergoes a rapid transition between two stabilized radii

necessarily induces a correlated step in G4D

Transition of the Effective Cosmological Constant

$$\tilde{\gamma}_{\rm p} = \tilde{\Lambda} - \frac{n(n-1)}{2}\frac{k_{\rm int}}{s_{\rm p}^2} \quad \text{for} \quad t < t_\dagger,$$

$$\tilde{\gamma}_0 = \tilde{\Lambda} - \frac{n(n-1)}{2}\frac{k_{\rm int}}{s_0^2} \quad \text{for} \quad t \geq t_\dagger.$$

Transition of the Gravitational constant G_{4D}

$$\frac{\left(\frac{\tilde{\kappa}}{\kappa}\right)_{\rm p}}{\left(\frac{\tilde{\kappa}}{\kappa}\right)_0} = \frac{G_{\rm 4D0}}{G_{\rm 4Dp}} = \left(\frac{s_{\rm p}}{s_0}\right)^n.$$

The Unifying Relation

$$\frac{G_{\rm 4D0}}{G_{\rm 4Dp}} = \left(\frac{s_{\rm p}}{s_0}\right)^n = \left(\frac{\tilde{\Lambda} - \tilde{\gamma}_0}{\tilde{\Lambda} - \tilde{\gamma}_{\rm p}}\right)^{n/2}.$$

$$\int_{\tilde{\rho}(t_1)}^{\tilde{\rho}(t_2)} \frac{\mathrm{d}\tilde{\rho}'}{\tilde{\rho}'} = -3\int_{a(t_1)}^{a(t_2)} \frac{\mathrm{d}a'}{a'} - n\int_{t_1}^{t_2} \mathrm{d}t \frac{\dot{s}}{s}\left[1 + \tilde{w}_{\rm int}(s)\right],$$

$$\tilde{\rho}_{\rm m}(t) = \begin{cases} \tilde{\rho}_{\rm mp} a(t)^{-3} & \text{for} \quad t < t_\dagger \\ \tilde{\rho}_{\rm m0} a(t)^{-3} & \text{for} \quad t \geq t_\dagger \end{cases}$$

$$\tilde{\rho}_{\rm mp} = \tilde{\rho}_{\rm m0}\left(\frac{s_0}{s_{\rm p}}\right)^{n\left[1+\tilde{w}_{\rm int}(t_\dagger^+)\right]},$$

$$\frac{\tilde{\Omega}_{\rm mp}}{\tilde{\Omega}_{\rm m0}} \equiv \frac{\tilde{\rho}_{\rm mp}}{\tilde{\rho}_{\rm m0}} \quad \text{along with} \quad \frac{\tilde{\Omega}_{\tilde{\gamma}\rm p}}{\tilde{\Omega}_{\tilde{\gamma}0}} \equiv \frac{\tilde{\gamma}_{\rm p}}{\tilde{\gamma}_0}.$$

$$\rho_{\rm mp} = \rho_{\rm m0} = \text{const.} \quad \text{and} \quad \tilde{w}_{\rm int}(t_\dagger^+) = 0.$$

VIABLE TRANSITION MODELS

TABLE I. Classification of transition models in terms of α.

$\alpha \equiv \tilde{\gamma}_{\rm p}/\tilde{\gamma}_0$	**Model**
1	higher-dimensional ΛCDM with static s
$(0,1)$	Magnitude change only, no sign change
0	Sudden Appearance of $\tilde{\gamma}_0$ at $t_\dagger$, $0 \to$ dS transition
$(-1,0)$	Sign change, AdS $\to$ dS transition
-1	Sign switch, Mirror AdS $\to$ dS transition - $\Lambda_{\rm s}$CDM

Mirror AdS-dS transition: $\alpha = -1$

$$\alpha = \frac{\tilde{\gamma}_{\rm p}}{\tilde{\gamma}_0} \equiv \frac{\tilde{\Omega}_{\tilde{\gamma}{\rm p}}}{\tilde{\Omega}_{\tilde{\gamma}0}},$$

IS INTERNAL SPACE CLOSED OR OPEN ?

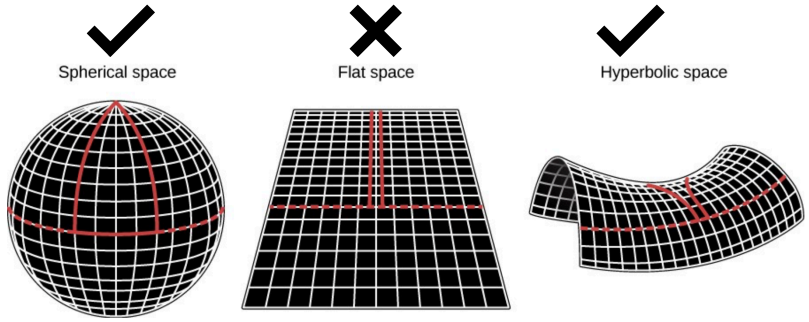

Figure 5. Picturing Space Curvature for the Entire Universe: The density of matter and energy determines the overall geometry of space. If the density of the universe is greater than the critical density, then the universe will ultimately collapse and space is said to be closed like the surface of a sphere. If the density exactly equals the critical density, then space is flat like a sheet of paper; the universe will expand forever, with the rate of expansion coming to a halt infinitely far in the future. If the density is less than critical, then the expansion will continue forever and space is said to be open and negatively curved like the surface of a saddle (where more space than you expect opens up as you move farther away). Note that the red lines in each diagram show what happens in each kind of space—they are initially parallel but follow different paths depending on the curvature of space. Remember that these drawings are trying to show how space for the entire universe is "warped"—this can't be seen locally in the small amount of space that we humans occupy.

$\Lambda_{\rm s}$CDM ΛCDM $\Lambda_{\rm s}$CDM

$$\tilde{\gamma}_{\rm p} = \tilde{\Lambda} - \frac{n(n-1)}{2}\frac{k_{\rm int}}{s_{\rm p}^2} \quad \text{for} \quad t < t_\dagger,$$

$$\tilde{\gamma}_0 = \tilde{\Lambda} - \frac{n(n-1)}{2}\frac{k_{\rm int}}{s_0^2} \quad \text{for} \quad t \geq t_\dagger.$$

$$\tilde{\Lambda} = \frac{n(n-1)}{4} k_{\rm int}\left(\frac{1}{s_{\rm p}^2} + \frac{1}{s_0^2}\right).$$

$$\text{sgn}[\tilde{\Lambda}] = \text{sgn}[\,k_{\rm int}].$$

$k_{\rm int} > 0 \quad \to \quad s_{\rm p} < s_0 \quad \to \quad G_{\rm 4Dp} > G_{\rm 4D0}.$

$$\Delta G_{\rm 4D}/G_{\rm 4D0} \approx -0.05$$

$$\tilde{\Lambda} \approx (20n-1)\tilde{\gamma}_0 \quad , \quad s_{\rm p} \approx (1 - 1/20n)s_0.$$

$$s_{\rm p} = \frac{s_0}{\sqrt{\frac{4\tilde{\Lambda}s_0^2}{n(n-1)k_{\rm int}} - 1}},$$

$$s_0 > \sqrt{\frac{n(n-1)k_{\rm int}}{4\tilde{\Lambda}}}.$$

the internal space must EXPAND
over time, leading to a WEAKING of the gravitational force

$k_{\rm int} < 0 \quad \to \quad s_{\rm p} > s_0 \quad \to \quad G_{\rm 4Dp} < G_{\rm 4D0}.$

$$\Delta G_{\rm 4D}/G_{\rm 4D0} \approx 0.05$$

$$\tilde{\Lambda} \approx -(20n+1)\tilde{\gamma}_0 \quad , \quad s_{\rm p} \approx (1 + 1/20n)s_0$$

$$\sqrt{\frac{n(n-1)k_{\rm int}}{4\tilde{\Lambda}}} < s_0 < \sqrt{\frac{n(n-1)k_{\rm int}}{2\tilde{\Lambda}}},$$

the internal space must SHRINK
over time, leading to a STRENGHENING of the gravitational force

$$\tilde{\Lambda} = \Lambda_{\rm QFT} \sim l_{\rm Planck}^{-2},$$

Predicted change ON MAGNITUDE is minuscule YET WITH A SIGN CHANGE IN HD CC.

$$\ddot{\delta} + 2H(z)\dot{\delta} - 4\pi G_{\rm eff}\rho\delta = 0,$$

THE RAPID TRANSITION MAY ARISE FROM QUANTUM TUNNELING BETWEEN QUASI-STATIC COMPACTIFICATION BRANCHES

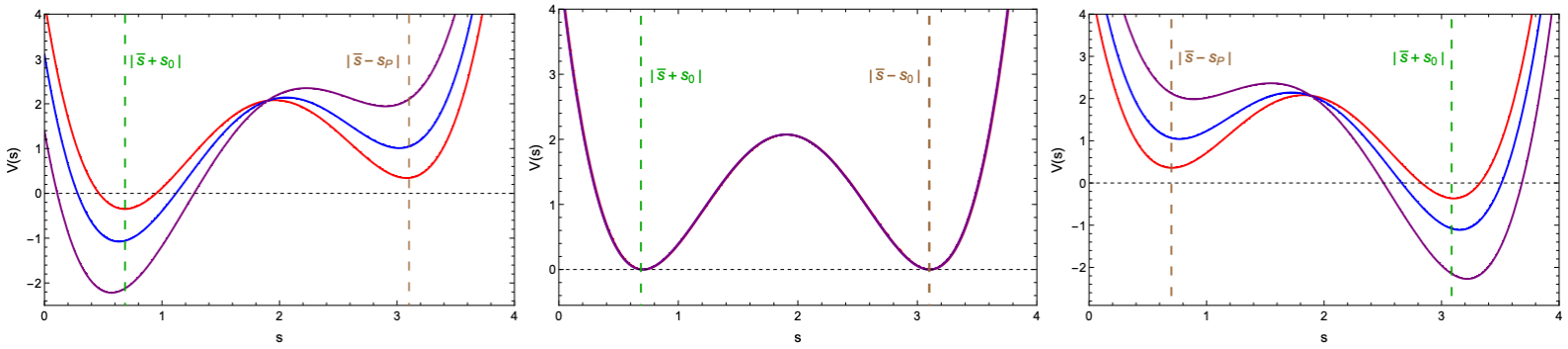

FIG. 2. Illustrative examples of the potential function $V(s)$ as a function of the internal scale factor s for different internal space dimensions n. The red, blue, and purple curves correspond to $n = 2$, $n = 3$, and $n = 4$, respectively, with parameters $s_0 = 1.2$ and $\bar{s} \sim 1.9$. The potential attains its minima at $s = |s_0 + \bar{s}|$ and $s = |-s_{\rm p} + \bar{s}|$, indicated by the vertical dark green and brown dashed lines respectively. **Left panel:** Negatively curved internal space ($k_{\rm int} = -1$). **Middle panel:** Flat internal space ($k_{\rm int} = 0$). **Right panel:** Positively curved internal space ($k_{\rm int} = 1$).

$$V(s) = \lambda\left[(s-\bar{s})^2 - s_0^2\right]^2 - n(n-1)\frac{k_{\rm int}}{\bar{s}^3}(s-\bar{s}),$$

$$:V(|\bar{s}-s_p|) > V(|\bar{s}+s_0|).$$

$$V_{\rm S}(s) = \lambda(s^2 - s_0^2)^2,$$

$$\left.\frac{dV}{ds}\right|_{s=s_*} = 4\lambda\left[(s_*-\bar{s})^2 - s_0^2\right](s_*-\bar{s}) - n(n-1)\frac{k_{\rm int}}{\bar{s}^3} = 0.$$

$$\bar{s} = \frac{s_0+s_p}{2} \pm \sqrt{\frac{(3s_0-s_p)(s_0+s_p)}{12}}, \qquad s_p/s_0 \le 3.$$

$$V_{\rm A}(s) = \epsilon(s-\bar{s}),$$

In every curvature case, sp is the false (higher-energy) vacuum and s0 the true (lower-energy) vacuum:

The transition is therefore always high→low energy, spontaneous and physically natural.

$$V(s) = V_{\rm S} + V_{\rm A}.$$

Negative curvature (stable) → internal space contracts (sp>s0)

positive curvature (unstable) → it expands

THE INTERNAL RADIUS IS A MODULUS IN A DOUBLE WELL WHOSE ASYMMETRY IS SET BY CURVATURE ITSELF; SP IS THE FALSE VACUUM AND S0 THE TRUE VACUUM, SO THE TRANSITION CAN HAPPEN SPONTANEOUSLY

Stability Conditions in static case

Internal space is open

We have to check the stability of this exact solution considering linear perturbations $\delta_{\rm ext}(t)$, $\delta_{\rm int}(t)$ and $\delta(t)$ about the backgrounds

$$\begin{aligned}\mathfrak{a}(t) =& a(t)[1+\delta_{\rm ext}(t)],\\ \mathfrak{s}(t) =& s(t)[1+\delta_{\rm int}(t)],\\ \tilde{\varrho}(t) =& \tilde{\rho}(t)[1+\delta(t)],\end{aligned}$$

$$\dot{\delta}+3\dot{\delta}_{\rm ext}+\frac{n}{2}\dot{\delta}_{\rm int}=0,$$

A system analogous to three springs connected in series, where the total length of the system remains constant

$$X_1+X_2+X_3=C.$$

$$\delta(t)+3\delta_{\rm ext}(t)+\frac{n}{2}\delta_{\rm int}(t)=C.$$

$$\left(\frac{{\rm d}^2}{{\rm d}t^2}+3H_{\rm ext}(t)\frac{\rm d}{{\rm d}t}+\omega_0^2\right)\delta_{\rm int}(t)=0,$$

oscillating with a real natural frequency

$$\omega_0=2\sqrt{\frac{\tilde{\chi}}{n}}=\frac{\sqrt{-2(n-1)k_{\rm int}}}{s_*}.$$

The stability condition is *at least two dimensional internal space*

$$k_{\rm int}<0, \quad \text{and} \quad n\neq 1,$$

$$\tilde{\gamma}=\tilde{\Lambda}+\frac{n\omega_0^2}{4}.$$

✓

Hyperbolic space

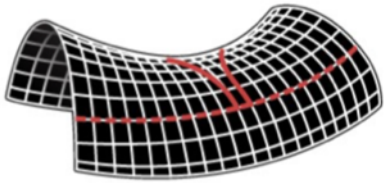

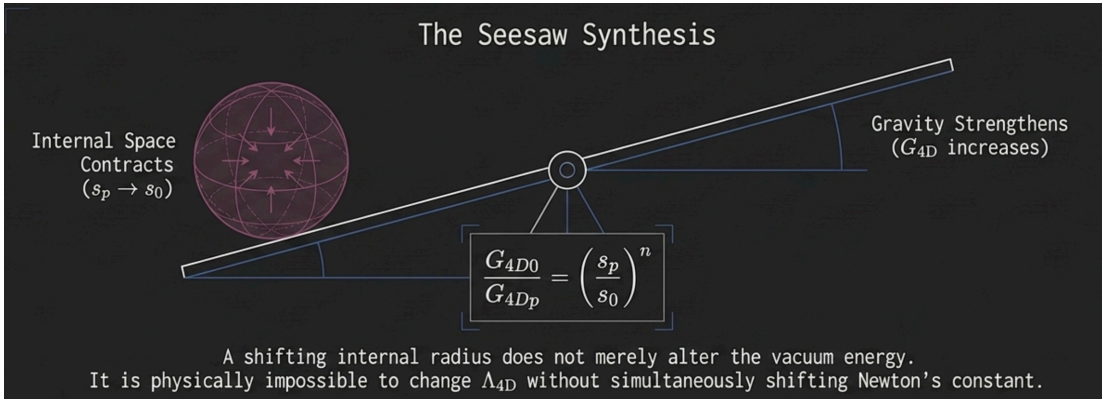

Akarsu & Dereli GRG 45 959 2013 1210.1155

J. G. Ratcliffe, Foundations of hyperbolic manifolds (Springer, New York, 2006)

Positive internal curvature naturally corresponds to compact simply-connected spaces, ***negative or vanishing curvature does not imply non-compactness: compact manifolds exist for any curvature sign once non-trivial global topology is allowed.***
One may construct compact hyperbolic manifolds of the form $\mathcal{K}^n=\mathcal{H}^n/\Gamma$, where $\mathcal{H}^n$ is n-dimensional hyperbolic space and Gamma is a discrete subgroup of its isometry group.

A schematic illustration of the roles of curvature $R^{\alpha}{}_{\beta\mu\nu}$, torsion $T^{\alpha}{}_{\mu\nu}$ and non-metricity $Q_{\alpha\mu\nu}$

Taken from Teleparallel gravity: from theory to cosmology, Rept. Prog. Phys. \textbf{86} (2023), 026901 2106.13793

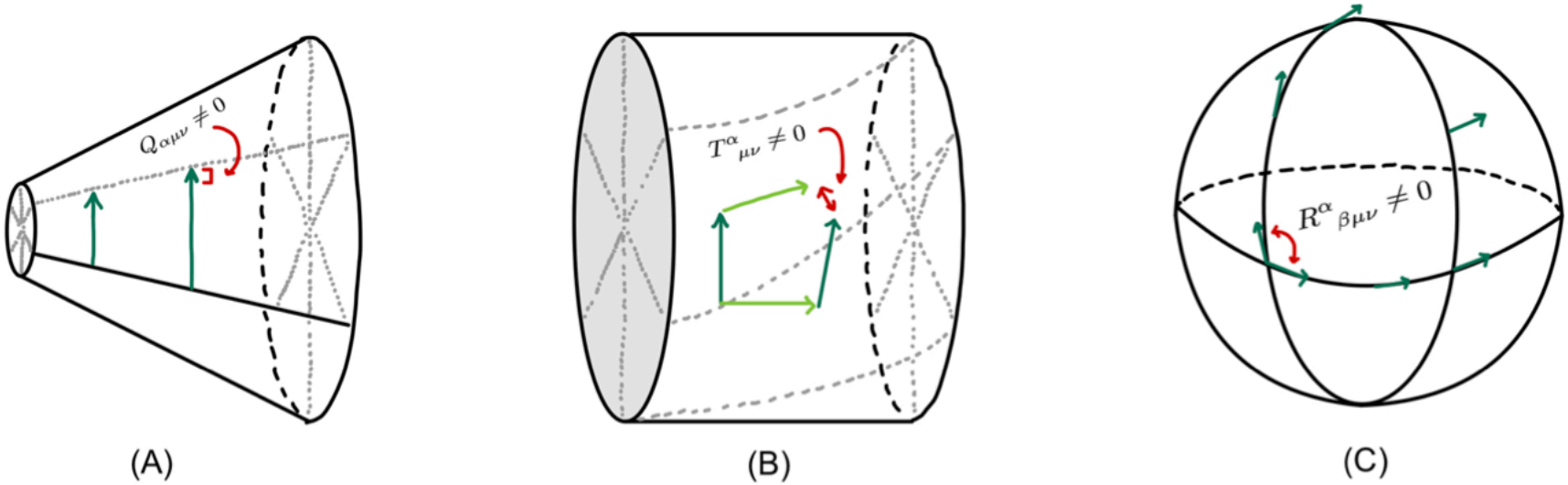

Non metricity (changing lengths)	Torsion (non closing)	Curvature (Rotation)

Jimenez,Heisenberg and Koivisto, ``The Geometrical Trinity of Gravity,'' Universe \textbf{5} (2019) 173. [arXiv:1903.06830 [hep-th]].

non-metricity changes the norm of vector fields transported along a curve

In the presence of torsion, parallelograms do not close.

If the space–time contains curvature, then the direction of a vector field changes when we move it along a closed circle

Teleparallel gravity : $R^{\alpha}{}_{\beta\mu\nu}=0$, $Q_{\alpha\mu\nu}=0$ and $T^{\alpha}{}_{\mu\nu} \neq 0$

For sure, we are free to introduce new geometric structures, such as yet another connection or, equivalently, the torsion and/or the nonmetricity tensors. However, it is strange to do so without influencing the physical predictions. The philosophy of trinity is based on an erroneous idea that the Levi-Civita connection was just an arbitrary choice. 2411.14089

Unexplored regions in teleparallel gravity : sign changing dark energy density

$$f(T) = Te^{\beta T_0/T}$$

Akarsu, Bulduk, De Felice, Katirci & Uzun, Phys. Rev. D 112, 083532 (2025) 2410.23068[gr-qc]

Awad, El Hanafy, Nashed & Saridakis, JCAP 02, 052 (2018). 1710.10194

Hashim, El Hanafy, Golovnev&El- Zant, JCAP 07, 052 (2021). 2010.14964 JCAP 07, 053 (2021). 2104.08311

Lets see $\beta < 0$?

$$\Omega_{\rm m0} = 2/\sqrt{e},$$

The negative exponent allows a transition to negative energy densities through torsional dark energy.

$$\rho_{\rm T}(z = z_\dagger) = 0,$$

Even we theoretically explore the uncharted regions of this model for the case predicting torsional dark energy featuring phantom behaviour.

$$3H^2 = \kappa\rho_{\rm m0}(1+z)^3 + \kappa\rho_{\rm T},$$

$$\rho_{\rm T}(H) = \frac{3H^2}{\kappa}\left[1 - \left(1 - 2\beta H_0^2/H^2\right)e^{\beta H_0^2/H^2}\right]$$

$$f_T = e^{\beta T_0/T}\left(1 - \beta T_0/T\right),$$
$$= e^{\beta H_0^2/H^2}\left(1 - \beta H_0^2/H^2\right),$$

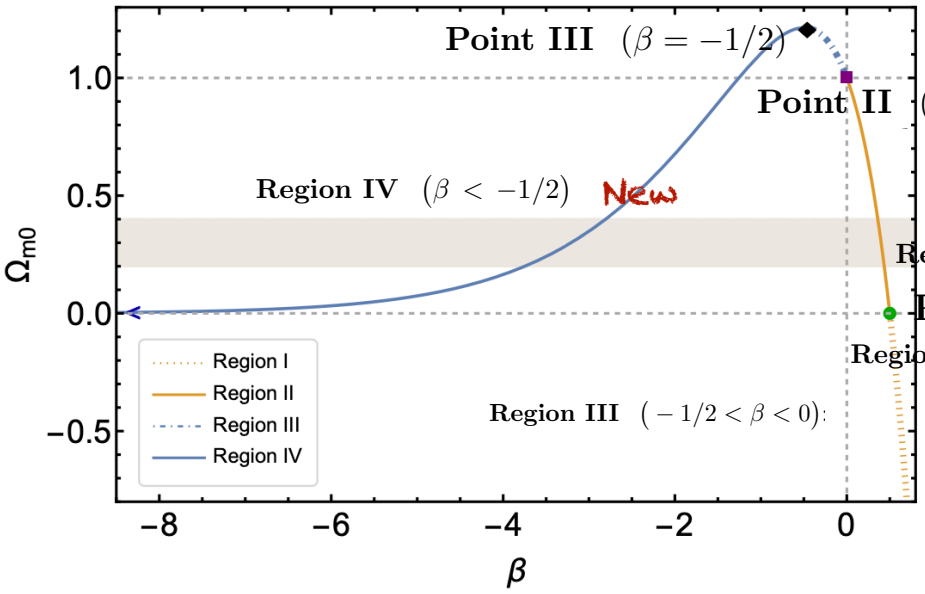

Matter dominated TEGR, Einstein-de Sitter Universe.

Empty universe however, a de Sitter background $H^2 = H_0^2$ due to the f(T) modification in the spacetime geometry even though no Λ is introduced.

Region I $(\beta > 1/2)$: $\Omega_{\rm m0} < 0$

Point I $(\beta = 1/2)$

Region II $(0 < \beta < 1/2)$ $0 < \Omega_{\rm m0} < 1$

This region also includes the observationally reasonable $\Omega_{\rm m0}$ interval shown by wheat band, however, it is overlooked in cosmological analyses in the literature to date.

- $\beta < 0$ is a sufficient condition to avoid instabilities/ghosts, you have $F_{\rm T} > 0$ independently of the value dynamics of T on any background, including the FLRW spacetime,

$$\ddot{\delta}_{\rm m} + 2H\dot{\delta}_{\rm m} - \frac{4\pi G_{\rm N}}{f_T}\rho_{\rm m}\delta_{\rm m} = 0\,,$$

- Conversely, when $\beta > 0$, one needs to ensure that dynamically the universe never entered through an era during which $f_T < 0$.

Quantitative analysis

Akarsu, Bulduk, De Felice, Katirci & Uzun, Phys. Rev. D 112, 083532 (2025) 2410.23068[gr-qc]

Awad, El Hanafy, Nashed & Saridakis, JCAP 02, 052 (2018). 1710.10194

Hashim, El Hanafy, Golovnev&El- Zant, JCAP 07, 052 (2021). 2010.14964 JCAP 07, 053 (2021). 2104.08311

$$f(T) \rightarrow f(T) + 2\Lambda$$

as z → ∞, H → 0, a Minkowski limit

as z → −1, then $H^2 \rightarrow 2\beta H_0^2$

Fixing $\theta_* = r_*/D_M(z_*)$

Utilizing from ΛCDM Planck18

constrained strictly/ almost model independently

through the measurement of Θ* (100Θ* = 1.041085)

$$\Omega_{m0}h^2 = 0.14314$$

the CMB-based constraint

$$D_M(z_*) = 13872.83 \text{ Mpc}$$

11

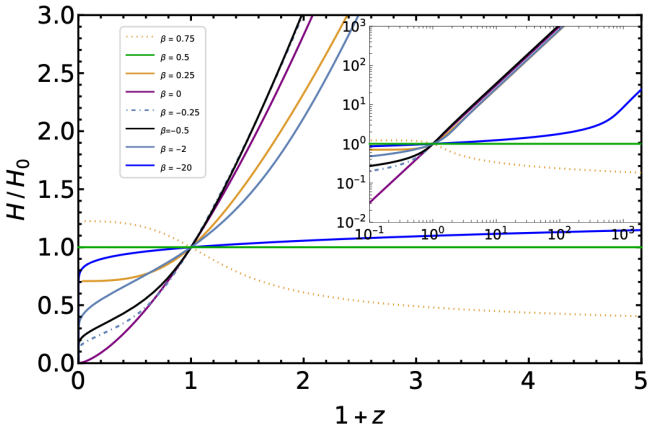

effective at post-recombination epoch

no effect on pre-recombination epoch

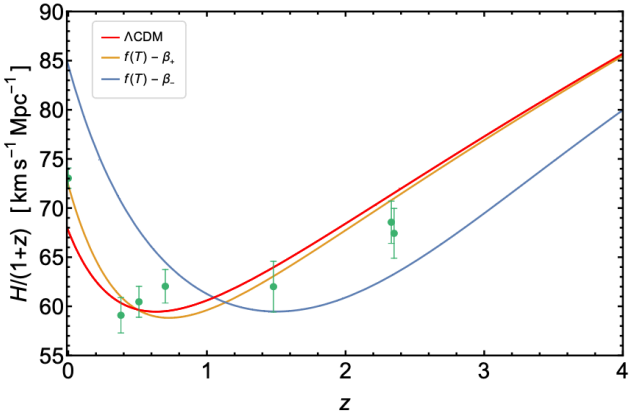

$$r_* = \int_{z_*}^{\infty} c_s \bar{H}^{-1} dz,$$

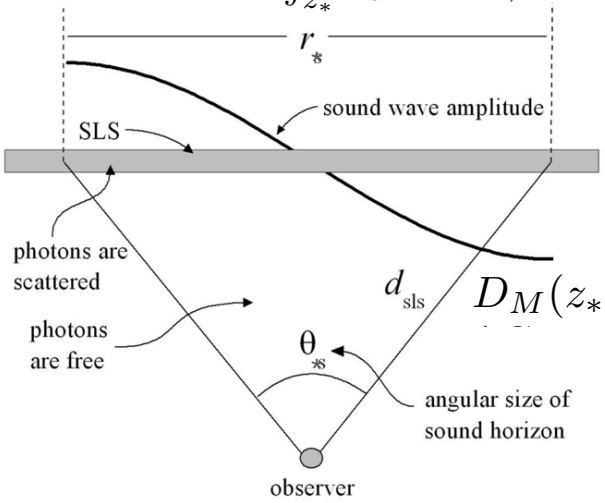

$$D_M(z_*) = \int_0^{z_*} cH^{-1} dz.$$

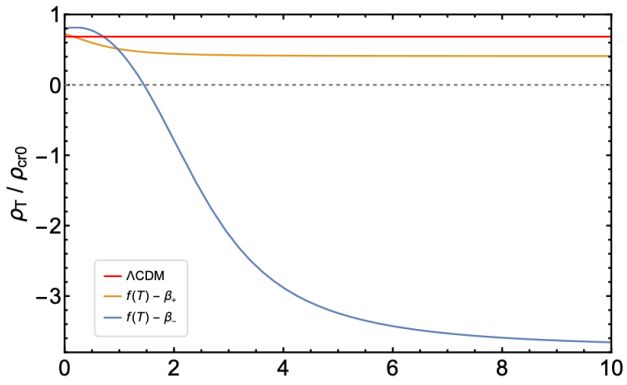

H0 = 68.86 km s−1Mpc−1, ΩM0 = 0.302 for ΛCDM model

H0 = 73.69 km s−1Mpc−1, ΩM0 = 0.264 and β+ = 0.413 within Region II

H0 = 85.66 km s Mpc , ΩM0 = 0.195 and β− = −3.782 within Region IV

QUANTITATIVE ANALYSIS

$$f(T) \rightarrow f(T) + 2\Lambda$$

$\dot{a} = H(z)/(1+z)$ (comoving Hubble parameter)

FIXING $\theta_* = r_*/D_M(z_*)$

UTILIZING FROM ΛCDM PLANCK18 CONSTRAINED STRICTLY/ ALMOST MODEL INDEPENDENTLY THROUGH THE MEASUREMENT OF Θ* (100Θ* = 1.041085)

$$\Omega_{m0}h^2 = 0.14314$$

THE CMB-BASED CONSTRAINT

$D_M(z_*) = 13872.83$ Mpc

EFFECTIVE AT POST-RECOMBINATION EPOCH
NO EFFECT ON PRE-RECOMBINATION EPOCH

$$r_* = \int_{z_*}^{\infty} c_s \bar{H}^{-1} dz,$$

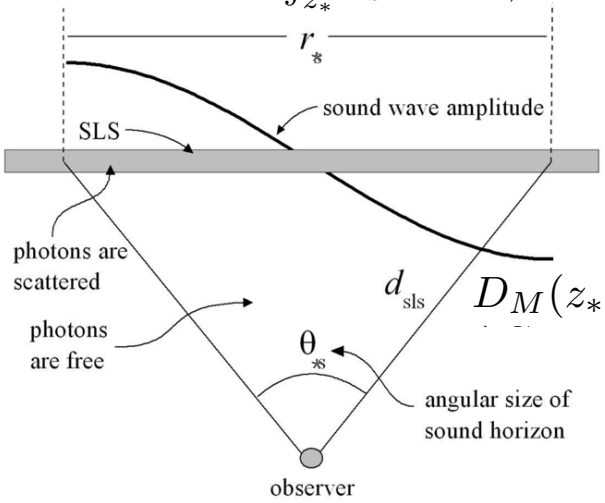

$$D_M(z_*) = \int_0^{z_*} cH^{-1} dz.$$

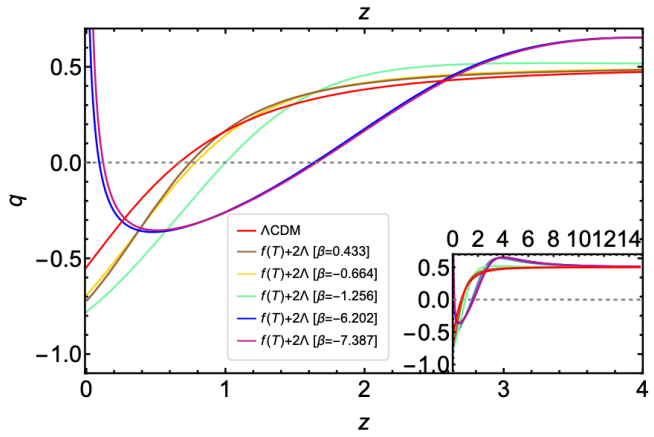

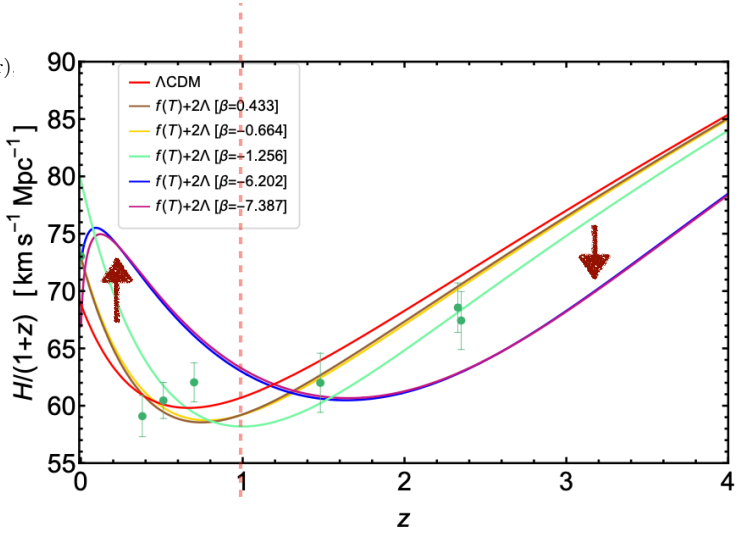

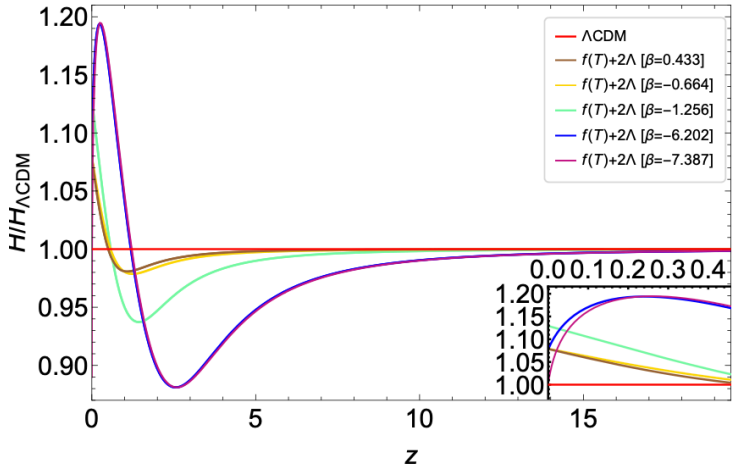

EXTENDING VIABLE COSMOLOGIES +
NOW WE HAVE LCDM LIMIT FOR β =0

h = H0/(100 km s^{-1}Mpc^{-1})

EXPONENTIAL INFRARED TELEPARALLEL MODEL WITH COSMOLOGICAL CONSTANT

$$f(T) \rightarrow f(T) + 2\Lambda$$

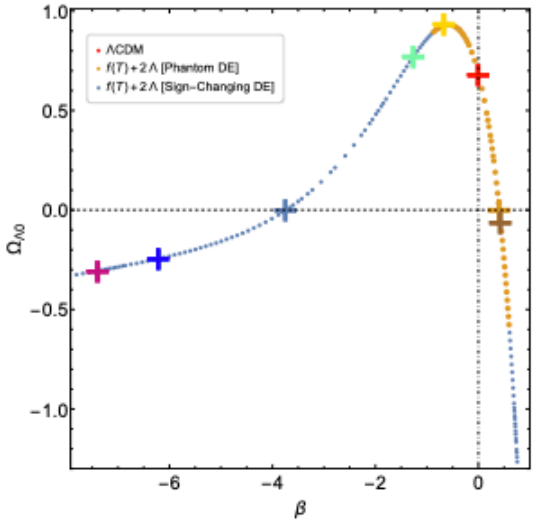

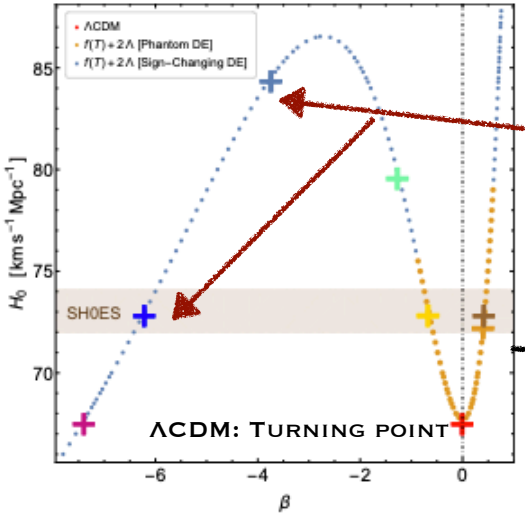

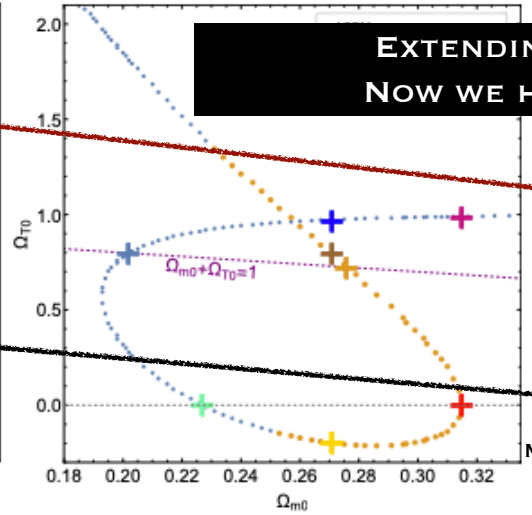

Extending viable cosmologies +
Now we have LCDM limit for β =0

$$\left(\frac{H^2}{H_0^2} - 2\beta\right) e^{\beta H_0^2/H^2} = \Omega_{\rm m0}(\beta,\Lambda)\,(1+z)^3 + \Omega_{\Lambda 0},$$

$$\Omega_{\rm m0}(\beta,\Lambda) = (1-2\beta)e^{\beta} - \Omega_{\Lambda 0},$$

THE EFFECT OF THE LARGE NEGATIVE IS MODERATED BY THE NEGATIVE VALUE OF Λ

MODELS SHOULD BE COMPARED WITH BAYESIAN ANALYS

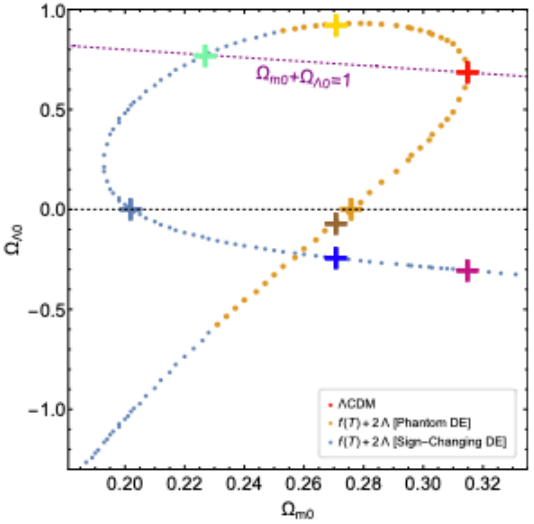

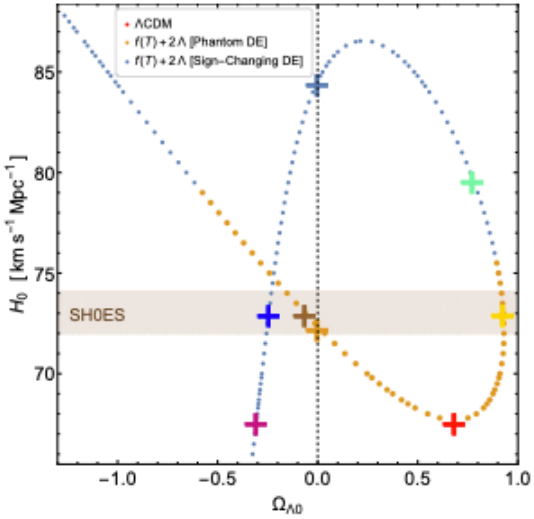

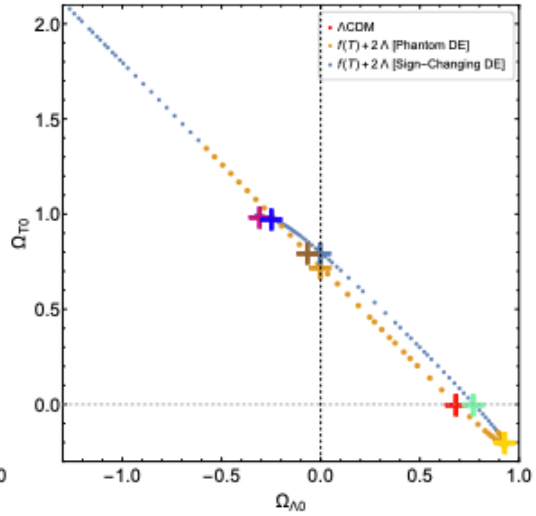

THE POINTS CORRESPOND TO MODELS HAVING PARAMETER SETS {H0, ΩM0, ΩΛ0, β} THAT SATISFY DM(z∗) = 13872.83 MPC CONSTRAINED STRICTLY AND ALMOST MODEL INDEPENDENTLY THROUGH THE MEASUREMENT OF Θ∗ (100Θ∗ = 1.041085) AND THE CMB-BASED CONSTRAINT $\Omega_{M0}h^2$ = 0.14314 ON THE PHYSICAL ENERGY DENSITY.

THE DOTTED PURPLE LINE IN THE RIGHT PANEL REPRESENTS ΩM0 + ΩΛ0 = 1.

$\Omega_{\Lambda 0} < 0$

REMARK I : PURPLE PLUS SIGN REPRESENTS THE MODEL IN LINE WITH FINDINGS FROM DESI PAPER GIVEN IN CALDERON, ET AL. 2405.04216 THAT ADDS AN EXTENSIVE CLASS OF MODEL-AGNOSTIC RECONSTRUCTIONS WITH ACCEPTABLE FITS TO THE DATA, INCLUDING MODELS WHERE COSMIC ACCELERATION SLOWS DOWN AT LOW REDSHIFTS.

REMARK II: STANDARD ΛCDM MODEL (RED PLUS) CORRESPONDS TO A VERY SPECIAL POINT, NAMELY, TO A LOCAL MINIMUM IN THE LEFT AND MIDDLE PANELS.

SHOES COLLABORATION MEASUREMENT H0 = 73.04 ± 1.04 KM S^{-1}MPC^{-1}

RIESS ET AL. ASTROPHYS. J. LETT. 934, L7 (2022) 2112.04510

Concluding remarks

✓ *Sign switching Λ can be generated by geometrical extensions of GR.*

✓ *effectively negative energy densities ARE NOT PROBLEMATIC, EVEN PROMISING.*

✓ *the change of gravitational constant can be used to a smoking gun for Λ_sCDM models realized through extra dımensions.*

✓*Along the way, we made unexpected signatures about the nature of dark energy cosmic slowing down at low redshifts.*

✓*CPL parametrization can not attain negative energy densities, therefore its succees is based on the sign changing its inertial mass density (IMD), is it fake or side effect due to not having negative energy densities?*

$$\varrho = \rho + p$$

✓ *Vacuum energy density may not be fundamental, what about inertial mass density?* Relativistic generalized inertia, Capozziello, Nazari & Katirci, ongoing work

✓ *If DE energy density changes its sign, w does not say anything, we should focus on IMD*

Null energy condition boundary crossing, 2602.21169, 2602.08928, 2603.15868

$$\rho + p = 0$$

✓ *Phantom/quintessence with posıtıve/negative energy density ???*

✓ *G4 terms may contribute to negative DE density in Horndenski gravity, yet should be checked from stability point of view.*